

Parabolic Approximation & Relaxation for MINLP

ADRIAN GÖß^{*}, ROBERT BURLACU^{}, ALEXANDER MARTIN^{}

MARCH 24, 2025

ABSTRACT. We propose an approach based on quadratic approximations for solving general Mixed-Integer Nonlinear Programming (MINLP) problems. Specifically, our approach entails the global approximation of the epigraphs of constraint functions by means of paraboloids, which are polynomials of degree two with univariate quadratic terms, and relies on a Lipschitz property only. These approximations are then integrated into the original problem. To this end, we introduce a novel approach to compute globally valid epigraph approximations by paraboloids via a Mixed-Integer Linear Programming (MIP) model. We emphasize the possibility of performing such approximations a-priori and providing them in form of a lookup table, and then present several ways of leveraging the approximations to tackle the original problem. We provide the necessary theoretical background and conduct computational experiments on instances of the MINLPLib. As a result, this approach significantly accelerates the solution process of MINLP problems, particularly those involving many trigonometric or few exponential functions. In general, we highlight that the proposed technique is able to exploit advances in Mixed-Integer Quadratically-Constrained Programming (MIQCP) to solve MINLP problems.

ACKNOWLEDGMENTS

We thank the German Research Foundation (Deutsche Forschungsgemeinschaft, DFG) for their support within project A05 in the “Sonderforschungsbereich/Transregio 154 Mathematical Modelling, Simulation and Optimization using the Example of Gas Networks” with Project-ID 239904186. Further, we gratefully acknowledge the scientific support and HPC resources provided by the Erlangen National High Performance Computing Center (NHR@FAU) of the Friedrich-Alexander-Universität Erlangen-Nürnberg (FAU). The hardware is funded by the DFG.

^{*}CORRESPONDING AUTHOR

(A. Göß, R. Burlacu, A. Martin) UNIVERSITY OF TECHNOLOGY NUREMBERG (UTN),
ANALYTICS & OPTIMIZATION LAB, DR.-LUISE-HERZBERG-STR. 4, 90461 NUREMBERG, GERMANY

E-mail address: {adrian.goess, robert.burlacu, alexander.martin}@utn.de.

2010 Mathematics Subject Classification. 90C11, 90C20, 90C26, 90C30 .

Key words and phrases. mixed-integer nonlinear programming, mixed-integer linear programming, quadratic approximation, global optimization.

1. INTRODUCTION

We consider the problem

$$\min c(\mathbf{x}) \tag{1a}$$

$$\text{s.t. } f_j(\mathbf{x}) \leq y_j, \quad j \in J, \tag{1b}$$

$$\mathbf{x} \in \Omega, \tag{1c}$$

$$\mathbf{y} \in [\underline{\mathbf{y}}, \overline{\mathbf{y}}], \tag{1d}$$

where $\Omega = [\underline{\mathbf{x}}, \overline{\mathbf{x}}] \cap (\mathbb{Z}^p \times \mathbb{R}^{n-p}) \neq \emptyset$ for $p, n \in \mathbb{N}$ with $0 \leq p \leq n$ and $|J| < \infty$. We assume the functions $c, f_j : \mathbb{R}^n \rightarrow \mathbb{R}$ to be continuous on the domain $[\underline{\mathbf{x}}, \overline{\mathbf{x}}]$, $j \in J$. Note that we can assume linearity of the objective c by introducing a separate variable z , which is then minimized subject to $c(\mathbf{x}) \leq z$ and the remaining constraints. We assume the existence of integer variables throughout the paper, i.e., $p > 0$, unless otherwise stated. In general, we consider at least one function to be nonlinear and therefore we refer to (1) as a Mixed-Integer Nonlinear Programming (MINLP) problem or, simply, a Mixed-Integer Nonlinear Program (MINLP). The right-hand sides y_j are inserted for ease of presentation and do not pose a major limitation, as discussed later.

The solution methods for a MINLP can vary enormously depending on the properties of the functions involved. See [18] for an overview of global solution strategies (mainly for continuous variables) and [6] for a survey of the most common components of practical approaches for MINLP problems.

In the case that all functions involved are convex, the feasible set of the continuous relaxation of (1) is also convex. Consequently, this is typically referred to as a *convex* MINLP. Such problems are usually tackled using cutting methods, such as outer approximation [13] or extended cutting-plane methods [30], and decomposition schemes, such as generalized Benders decomposition [15].

However, if at least one of the functions is not convex, the situation changes, and (1) is then referred to as a *non-convex* MINLP. Typically, non-convex MINLP problems are solved by a combination of convex relaxation of the non-convex nonlinearities and a refinement mechanism. Effective convexification techniques are proposed by [28], among others. Since these may not provide a sufficiently tight representation of the original domain, the feasible region can be split to generate new subproblems with tighter convex relaxations. This divide-and-conquer approach is performed in spatial branch-and-bound by reformulation (see, e.g., [24]) or in α -branch-and-bound by α -convexification [3]. In the last decade, a viable alternative has received new attention, namely the approximation of the non-convex functions by piecewise linear functions and the subsequent reformulation as a Mixed-Integer Linear Programming (MIP) problem (alternatively, Mixed-Integer Linear Program (MIP)), particularly for real-world applications with considerable combinatorics [9, 14]. For a comprehensive overview of the theoretical properties of the various MIP-based models for piecewise linear functions, refer to [29].

A natural generalization of the piecewise linear approach is the piecewise approximation by polynomials of a certain degree. Such an approximation is performed in an optimization setting using quadratic functions [8]. In certain algebraic subfields, sets of more general polynomials of this type are usually referred to as *splines*, and a distinction is made between approximations with fixed and variable knots, i.e., discretization points of an interval. There is a vast amount of literature starting from the 1960s on splines. Nürnberger [23] gives a comprehensive review of the first approximately 30 years. For a more recent introduction to the topic, we refer the reader to [26].

From an optimization perspective, the piecewise approximation by higher-order polynomials instead of linear functions does not offer a clear advantage, as this implies the introduction of both non-convex constraints and integer variables. However, if we can perform a one-sided spline approximation, i.e., an underestimation of a function on its domain, this serves as a globally valid relaxation that does not require piecewise modeling. In other terms, the underestimation is an approximation of the epigraph of the function. In [7], the authors prove existence and uniqueness for a best one-sided approximation with maximum degree. A computational procedure to compute such an approximation with a single polynomial is presented in [19].

Surprisingly, we did not find any literature that treats the one-sided approximation by a spline with variable knots, as we require it for optimization. The existing research is either limited to spline approximations that are not one-sided (see [2] or again [26]), which does not yield a globally valid relaxation of the MINLP, or it focuses on best approximation by a single polynomial (see [12]).

In Section 2, we thus present an MIP model for the one-sided approximation by univariate quadratic functions and prove its correctness. In Section 3, we formally introduce the resulting method for approximating non-convex constraint functions by a small number of such quadratic functions and their integration into an MINLP. This is complemented by computational showcases in Section 4, and the article concludes with remarks and further research directions in Section 5.

1.1. Contribution. We propose a framework to solve optimization problems with general nonlinear constraints by employing multiple quadratic constraints, which fulfill a predefined approximation accuracy. To the best of our knowledge, there is no approach for solving MINLP problems that globally approximates non-convex functions on their respective domains to a given accuracy without introducing additional variables, i.e., increasing the dimension of the problem, or branching on continuous variables. In essence, this framework has the potential to turn an MINLP problem into an Mixed-Integer Quadratically-Constrained Programming (MIQCP) one such that a solution to the latter serves as an ε -approximate solution for the original problem. Thus, this approach enables to leverage recent advancements in MIQCP (see, for instance, [4, 5, 31]) to solve MINLP problems.

To this end, we present a novel approach to compute a globally valid one-sided approximation for nonlinear functions by means of polynomials of degree two with univariate quadratic terms only. This includes an MIP model, which basically relies on a Lipschitz property only, and several strategies to determine the number of approximating functions. Based on the results, we introduce techniques to incorporate such parabolic approximations in MINLP problems to provide dual bounds or even accelerate the solving of the original problem. The theoretical explanations are complemented with computational experiments on the MINLPLib [10], demonstrating limitations and potentials by this framework.

Lastly, we motivate the usage of a lookup table for approximations on generic domains when solving MINLP problems. This is possible through the properties of global validity and one-sidedness. Akin to the realm of Machine Learning, this accepts extensive a-priori computations and then compensates for them by repetitive use of the results.

1.2. Notation. A vector $\mathbf{x} = (x_1, \dots, x_n)^\top \in \mathbb{R}^n$ is denoted with bold and upright letters, whereas components x_i are italic and not bold. A comparison between two vectors $\mathbf{x}, \mathbf{z} \in \mathbb{R}^n$, e.g., $\mathbf{x} \leq \mathbf{z}$, is always interpreted component-wise. In the theoretical section, we make use of the 1-norm of a vector \mathbf{x} which is defined as $\|\mathbf{x}\|_1 = \sum_{i=1}^n |x_i|$. For a domain $\mathcal{D} \subseteq \mathbb{R}^n$, we define the set of continuous functions

on \mathcal{D} as $\mathcal{C}^0(\mathcal{D})$. Further, $\mathcal{P}(\mathcal{D})$ denotes the power set of \mathcal{D} . Lastly, for a positive integer $m \in \mathbb{N}$, we state the set of indexes up to m as $[m] := \{1, \dots, m\}$.

Note that we present our theoretical part for constraint functions on a multi-dimensional domain. We aim for their approximation by quadratic functions without bivariate terms and refer to such as *paraboloids*. Hence, the global one-sided approximation by paraboloids is called a *parabolic approximation*. Later on, when we substitute constraint functions with mentioned approximations, we name such a *parabolic relaxation*, emphasizing the character of this procedure.

2. PARABOLIC APPROXIMATION – MIP APPROACH

The term *one-sided* implies an approximation of the function's (hypo-/)epigraph, coining the expression of an approximation *from below (above)*. In this context, a set of paraboloids serves as a *global* approximation if every paraboloid is a underestimator(/overestimator) of the approximated function on its entire domain. In the following, we introduce an MIP model to compute such a global one-sided approximation given a fixed number $K \in \mathbb{N}$ of paraboloids and a Lipschitz function f together with its Lipschitz constant L . We also include the usage of a measure to compute the Lebesgue integral of f on a given domain. This is not necessary for the functionality of the model, but decreases its size, as mentioned in the respective paragraph.

Formally, let $f : \mathcal{D} \mapsto \mathbb{R}$ be a Lipschitz continuous function with respect to $\|\cdot\|_1$ and some $L > 0$, where $\mathcal{D} = [\mathbf{a}, \mathbf{b}]$ a non-empty, full dimensional box defined by the vectors $\mathbf{a}, \mathbf{b} \in \mathbb{R}^n$. That is, for all $\mathbf{x}, \mathbf{y} \in \mathcal{D}$, it holds true that

$$|f(\mathbf{x}) - f(\mathbf{y})| \leq L\|\mathbf{x} - \mathbf{y}\|_1.$$

Mentioning Lipschitz continuity in the remainder of this article, we will always refer to $\|\cdot\|_1$ if not stated otherwise. In addition, we assume to know a function $\mu_f : \mathcal{P}(\mathcal{D}) \mapsto \mathbb{R}_+$, measuring the Lebesgue integral of f on any connected sub-domain of \mathcal{D} . In the one-dimensional case, such a function is typically the anti-derivative of f .

Note that, f represents a constraint function f_j from (1). In this section, we exclusively treat its approximation from below, but remark that the approximation from above can be treated analogously by considering $-f$ instead.

For the approximation, we assume some guarantee $\varepsilon > 0$ to be given and aim to determine paraboloids $p^l(\mathbf{x})$ for $l \in [K]$ such that

$$\max_{l \in [K]} p^l(\mathbf{x}) \geq f(\mathbf{x}) - \varepsilon, \tag{C1}$$

and

$$\max_{l \in [K]} p^l(\mathbf{x}) \leq f(\mathbf{x}), \tag{C2}$$

for all $\mathbf{x} \in \mathcal{D}$. Condition (C1) ensures that $(p^l)_l$ serve in their entity as an approximation of the desired guarantee, whereas (C2) secures the one-sided property. In fact, one could reformulate it to $p^l(\mathbf{x}) \leq f(\mathbf{x})$ for all $l \in [K]$.

2.1. MIP Model. In the following model, we interpret the coefficients of the paraboloids as variables. If solved with an objective value of zero, the corresponding solution then determines paraboloids that satisfy conditions (C1) and (C2).

Before stating the model explicitly, we need to introduce the parameters $\delta \in (0, \varepsilon)$ and $\nu \in (0, \delta/\varepsilon)$. Informally, their choices influence the centering of the parabolic approximation inside the ε -tube between f and $f - \varepsilon$. This becomes clearer throughout this section. In addition, a constant $C \geq L$ needs to be chosen which bounds the maximal absolute slope of each paraboloid and thus controls their “spiking”.

With these parameters at hand, we define the widths Δt_i and Δd_i for $i \in [n]$ such that

$$\sum_{i=1}^n \Delta t_i \leq \frac{n+1}{n} \frac{\varepsilon - \delta}{3L}, \quad (2)$$

and

$$\Delta d_i \leq \frac{2\nu\varepsilon}{(\sqrt{3}-1)n(C+L)}. \quad (3)$$

Because the right-hand side of the above inequalities is strictly positive, such a choice is always possible. Without loss of generality, we can assume Δt_i and Δd_i to be chosen such that $(b_i - a_i)/\Delta t_i \in \mathbb{N}$ and $(b_i - a_i)/\Delta d_i \in \mathbb{N}$ for all $i \in [n]$. This allows to define two grids on the domain \mathcal{D} as

$$\mathcal{G}_\varepsilon := \bigtimes_{i=1}^n \left\{ a_i + k\Delta t_i \mid k = 0, 1, \dots, \frac{b_i - a_i}{\Delta t_i} \right\},$$

and

$$\mathcal{G} := \bigtimes_{i=1}^n \left\{ a_i + k\Delta d_i \mid k = 0, 1, \dots, \frac{b_i - a_i}{\Delta d_i} \right\}.$$

Constraints defined on these grids enforce the conditions (C1) and (C2), respectively. If we collect the individual grid widths as the vectors $\Delta \mathbf{t} = (\Delta t_1, \dots, \Delta t_n)^\top$ and $\Delta \mathbf{d} = (\Delta d_1, \dots, \Delta d_n)^\top$, we are able to rewrite the domain \mathcal{D} as

$$\mathcal{D} = \bigcup_{\mathbf{t} \in \mathcal{G}_\varepsilon \cap [\mathbf{a}, \mathbf{b})} [\mathbf{t}, \mathbf{t} + \Delta \mathbf{t}] = \bigcup_{\mathbf{d} \in \mathcal{G} \cap [\mathbf{a}, \mathbf{b})} [\mathbf{d}, \mathbf{d} + \Delta \mathbf{d}]. \quad (4)$$

Note that the arguments of each union intersect at most on their boundaries. For clear notation in the model, we abbreviate $\mathcal{B}(\mathbf{d}) = [\mathbf{d}, \mathbf{d} + \Delta \mathbf{d}]$. Further, we denote all neighboring points to \mathbf{t} in \mathcal{G}_ε , i.e., all points which differ in each coordinate by exactly Δt_i , as

$$\mathcal{N}(\mathbf{t}) = \left\{ \mathbf{t} + \sum_{i=1}^n u_i \Delta t_i \mathbf{e}_i \in \mathcal{G}_\varepsilon \mid \mathbf{u} \in \{-1, 1\}^n \right\},$$

where \mathbf{e}_i denotes the i th unit vector.

In terms of variables, we denote the paraboloid coefficients $\alpha_i^l, \beta_i^l, \gamma^l$ for $i \in [n]$ and $l \in [K]$, specifying the l th paraboloid as $p^l(\mathbf{x}) = \sum_{i=1}^n \alpha_i^l x_i^2 + \sum_{i=1}^n \beta_i^l x_i + \gamma^l$. Furthermore, we introduce binary variables $s_{\mathbf{t}}^l \in \{0, 1\}$ for all $l \in [K]$ and all grid points $\mathbf{t} \in \mathcal{G}_\varepsilon$. These indicate whether the l th paraboloid fulfills $p^l(\mathbf{t}) \geq f(\mathbf{t}) - \delta$, which is a slight variation to (C1) and ensures the latter. Condition (C2), however, is controlled by continuous variables $v_{\mathbf{d}}^l \geq 0$ for $l \in [K]$ and $\mathbf{d} \in \mathcal{G}$, which track violations of the integral between f and a paraboloid p^l .

Now, we can finally formulate the MIP. For a comprehensive presentation, nonlinear expressions are kept and their equivalent linear formulation is discussed afterwards.

$$\min \sum_{l \in [K]} \sum_{\mathbf{d} \in \mathcal{G} \cap [\mathbf{a}, \mathbf{b})} v_{\mathbf{d}}^l \quad (5a)$$

$$\text{s.t.} \quad p^l(\mathbf{t}) \geq f(\mathbf{t}) - \delta - M_1(1 - s_{\mathbf{t}}^l), \quad l \in [K], \mathbf{t} \in \mathcal{G}_\varepsilon, \quad (5b)$$

$$\sum_{l \in [K]} s_{\mathbf{t}}^l \geq 1, \quad l \in [K], \mathbf{t} \in \mathcal{G}_\varepsilon, \quad (5c)$$

$$\left| \frac{d}{dx_i} p^l(\mathbf{t}') \right| \leq 2L + M_2(1 - s_{\mathbf{t}}^l), \quad l \in [K], i \in [n], \mathbf{t} \in \mathcal{G}_\varepsilon, \mathbf{t}' \in \mathcal{N}(\mathbf{t}), \quad (5d)$$

$$p^l(\mathbf{d}) \leq f(\mathbf{d}) - \nu\varepsilon, \quad l \in [K], \mathbf{d} \in \mathcal{G}, \quad (5e)$$

$$v_{\mathbf{d}}^l \geq \int_{\mathcal{B}(\mathbf{d})} p^l(\mathbf{x}) - (f(\mathbf{x}) - \nu\varepsilon) d\mathbf{x}, \quad l \in [K], \mathbf{d} \in \mathcal{G}, \quad (5f)$$

$$\left| \frac{d}{dx_i} p^l(\mathbf{a}) \right| \leq C, \quad l \in [K], i \in [n], \quad (5g)$$

$$\left| \frac{d}{dx_i} p^l(\mathbf{b}) \right| \leq C, \quad l \in [K], i \in [n], \quad (5h)$$

$$\alpha_i^l, \beta_i^l, \gamma^l \in \mathbb{R}, \quad l \in [K], i \in [n], \quad (5i)$$

$$s_{\mathbf{t}}^l \in \{0, 1\}, \quad l \in [K], \mathbf{t} \in \mathcal{G}_\varepsilon, \quad (5j)$$

$$v_{\mathbf{d}}^l \geq 0, \quad l \in [K], \mathbf{d} \in \mathcal{G}. \quad (5k)$$

Since $\frac{d}{dx_i} p^l(\mathbf{x}) = 2\alpha_i^l x_i + \beta_i^l$ for $l \in [K]$, the derivative from above is a linear expression in the variables α_i^l and β_i^l . Further, for a function $h(\mathbf{x}) : \mathcal{D} \mapsto \mathbb{R}$, we rewrite $|h(\mathbf{x})| \leq C$ as $h(\mathbf{x}) \leq C$ and $h(\mathbf{x}) \geq -C$. This allows to rewrite constraints (5d), (5g), and (5h) as linear inequalities. Similarly, the anti-derivative of p^l is a linear term in the variables α_i^l , β_i^l and γ^l . Combined with μ_f the integral in (5f) is evaluated and the constraints reduce to another set of linear inequalities. This concludes the formulation of the problem by means of MIP techniques.

2.2. Existence & Validity of a Solution. We have to show two aspects regarding model (5): the existence of a solution for appropriate choice of parameters and the validity of conditions (C1) and (C2) for such a solution. The following theorem provides the first one.

Theorem 2.1 (Existence). *Let $0 < \Delta \leq \min\{\frac{n+1}{n^2} \frac{\varepsilon - \delta}{3L}, \frac{2\nu\varepsilon}{(\sqrt{3}-1)n(C+L)}, \frac{2\delta}{nL}\}$. Further, assume that $\Delta d_i = \Delta t_i = \Delta$ for all $i \in [n]$, $C = 2L\|\mathbf{b} - \mathbf{a}\|_\infty / \Delta$, and $\nu = \delta / (2\varepsilon)$. Then, for*

$$K = |\mathcal{G}_\varepsilon| = \prod_{i=1}^n \left\lceil \frac{b_i - a_i}{\Delta} \right\rceil,$$

problem (5) has an optimal solution with an objective value of zero.

Proof. A detailed proof can be found in Appendix A.1. \square

Before turning to the validity of a solution, we demonstrate a connection between bounds to the partial derivatives and the Lipschitz continuity of a paraboloid.

Lemma 2.2. *Let $p(\mathbf{x}) = \sum_{i=1}^n \alpha_i x_i^2 + \sum_{i=1}^n \beta_i x_i + \gamma$ be a paraboloid and $\mathcal{D}' = [\mathbf{a}', \mathbf{b}']$. If there exists $C > 0$ such that*

$$\left| \frac{d}{dx_i} p(\mathbf{a}') \right| \leq C \quad \wedge \quad \left| \frac{d}{dx_i} p(\mathbf{b}') \right| \leq C,$$

it follows that

$$\forall \mathbf{x} \in \mathcal{D}' : \left| \frac{d}{dx_i} p(\mathbf{x}) \right| \leq C,$$

for all $i \in [n]$. Further, p is Lipschitz continuous on \mathcal{D}' with Lipschitz constant nC with respect to $\|\cdot\|_\infty$ and with Lipschitz constant C with respect to $\|\cdot\|_1$.

Proof. A detailed proof can be found in Appendix A.2. \square

The lemma shows that the bounds in (5g) and (5h) directly force a paraboloid defined by a feasible solution to be Lipschitz continuous with constant C . Additionally, inequalities (5d) ensure that a paraboloid p^l with $s_{\mathbf{t}}^l = 1$ is Lipschitz continuous on the neighborhood $\mathcal{N}(\mathbf{t})$ of \mathbf{t} with constant $2L$.

Combining this implied Lipschitz continuity of a paraboloid with the Lipschitz continuity of f turns the difference of both into a Lipschitz function itself. We leverage this effect to prove bounds on this difference, while abstracting the situation. We begin by establishing a lower bound based on the Lipschitz property and non-negativity on the vertices of a given domain.

Lemma 2.3. *Let $g \in \mathcal{C}^0(\mathcal{D}')$ be Lipschitz continuous with constant $L_g > 0$ and $\mathcal{D}' = [\mathbf{a}', \mathbf{b}'] \subseteq \mathcal{D}$. If $g(\mathbf{v}) \geq 0$ for all vertices \mathbf{v} of \mathcal{D}' , then it holds true that*

$$\min_{\mathbf{x} \in \mathcal{D}'} g(\mathbf{x}) \geq -\frac{L_g n}{n+1} \|\mathbf{b}' - \mathbf{a}'\|_1.$$

Proof. A detailed proof can be found in Appendix A.3. \square

Note that this result provides an analogous upper bound to $\max_{\mathbf{x} \in \mathcal{D}'} g(\mathbf{x})$ when assuming $g(\mathbf{v}) \leq 0$, respectively. This would already suffice to construct an MIP which provably returns a solution that satisfies (C1) and (C2) if the objective value is zero. However, we have included the availability of a Lebesgue measure to be able to evaluate the integral in (5f), which can be leveraged to improve such bounds. In the following lemma, this is demonstrated.

Lemma 2.4. *Let $g \in \mathcal{C}^0(\mathcal{D}')$ be Lipschitz continuous with constant $L_g > 0$ and $\mathcal{D}' = [\mathbf{a}', \mathbf{b}'] \subseteq \mathcal{D}$ full dimensional. If $g(\mathbf{v}) \leq 0$ for all vertices \mathbf{v} of \mathcal{D}' and $\int_{\mathcal{D}'} g(\mathbf{x}) d\mathbf{x} \leq 0$, then it holds true that*

$$\max_{\mathbf{x} \in \mathcal{D}'} g(\mathbf{x}) \leq \frac{\sqrt{3}-1}{2} \Delta_{\max} n L_g,$$

where $\Delta_{\max} = \max_{i \in [n]} b'_i - a'_i$.

Proof. A detailed proof can be found in Appendix A.4. \square

To get a feeling for the magnitudes of both bounds, let's consider an approximately cubic domain, in particular, roughly equidistant along each coordinate such that $\|\mathbf{b}' - \mathbf{a}'\|_1 \approx n \Delta_{\max}$. Then, it remains to notice that $0.366 \approx (\sqrt{3}-1)/2 < n/(n+1)$ for all $n \in \mathbb{N}$. We remark that the bound is tighter in any case for $n = 1$ and in cases of approximately cubic domains also for $n \geq 2$.

Now, Lemma 2.3 and Lemma 2.4 are leveraged in combination with Lemma 2.2 to show that a solution of (5) with zero objective satisfies (C1) and (C2), respectively. We start with the former case.

Theorem 2.5 (Validity of (C1)). *If $(\alpha_i^l, \beta_i^l, \gamma^l)$, $s_{\mathbf{t}}^l$, for $\mathbf{t} \in \mathcal{G}_\varepsilon$, $l \in [K]$, $i \in [n]$, satisfy the constraints (5b) to (5d), then the paraboloids $(p^l)_{l \in K}$ defined by the parameters $(\alpha_i^l, \beta_i^l, \gamma^l)$ fulfill (C1).*

Proof. Recall from (4) that \mathcal{D} is the union of $[\mathbf{t}, \mathbf{t} + \Delta \mathbf{t}]$ over all $\mathbf{t} \in \mathcal{G}_\varepsilon \cap [\mathbf{a}, \mathbf{b}]$. Hence, consider an arbitrary but fixed $\mathbf{t} \in \mathcal{G}_\varepsilon \cap [\mathbf{a}, \mathbf{b}]$ and the box $[\mathbf{t}, \mathbf{t} + \Delta \mathbf{t}]$.

Observe that all vertices \mathbf{t}' of $[\mathbf{t}, \mathbf{t} + \Delta \mathbf{t}]$ are again vectors in \mathcal{G}_ε . Therefore, (5c) with the integrality restriction on $s_{\mathbf{t}}^l$ ensure that for all such \mathbf{t}' , there exists $l \in [K]$ such that $s_{\mathbf{t}'}^l = 1$. We collect these indices in

$$I_{\mathbf{t}} = \{l \in [K] \mid \exists \mathbf{t}' \text{ vertex of } [\mathbf{t}, \mathbf{t} + \Delta \mathbf{t}] : s_{\mathbf{t}'}^l = 1\}.$$

Now, for all $l \in I_{\mathbf{t}}$, the inequalities (5d) in combination with Lemma 2.2 ensure that paraboloid p^l is Lipschitz continuous on $[\mathbf{t}, \mathbf{t} + \Delta \mathbf{t}]$ with constant $2L$. Indeed, we can show that this Lipschitz property transfers to $\max_{l \in I_{\mathbf{t}}} p^l(\mathbf{x})$. To this end, consider $\mathbf{x}, \mathbf{y} \in [\mathbf{t}, \mathbf{t} + \Delta \mathbf{t}]$ and let $l_{\mathbf{x}} \in \arg \max_{l \in I_{\mathbf{t}}} p^l(\mathbf{x})$, as well as $l_{\mathbf{y}} \in \arg \max_{l \in I_{\mathbf{t}}} p^l(\mathbf{y})$. If $p^{l_{\mathbf{x}}}(\mathbf{x}) \geq p^{l_{\mathbf{y}}}(\mathbf{y})$, we can derive

$$|\max_{l \in I_{\mathbf{t}}} p^l(\mathbf{x}) - \max_{l \in I_{\mathbf{t}}} p^l(\mathbf{y})| = |p^{l_{\mathbf{x}}}(\mathbf{x}) - p^{l_{\mathbf{y}}}(\mathbf{y})| = p^{l_{\mathbf{x}}}(\mathbf{x}) - p^{l_{\mathbf{y}}}(\mathbf{y})$$

$$\leq p^{l^*}(\mathbf{x}) - p^{l^*}(\mathbf{y}) \leq |p^{l^*}(\mathbf{x}) - p^{l^*}(\mathbf{y})| \leq 2L\|\mathbf{x} - \mathbf{y}\|_1,$$

where we used the fact $p^{l^*}(\mathbf{y}) \geq p^l(\mathbf{y})$ for all $l \in I_{\mathbf{t}}$. The case $p^{l^*}(\mathbf{x}) \leq p^l(\mathbf{y})$ follows analogously. Now, define $g(\mathbf{x}) := \max_{l \in I_{\mathbf{t}}} p^l(\mathbf{x}) - (f(\mathbf{x}) - \delta)$. The above result and the Lipschitz property of f give by the triangle inequality that g is Lipschitz continuous with constant $L_g = 2L + L = 3L$.

In addition, for all vertices \mathbf{t}' of $[\mathbf{t}, \mathbf{t} + \Delta\mathbf{t}]$, there exists $l \in I_{\mathbf{t}}$ with $s_{\mathbf{t}'}^l = 1$ and by (5b) $p^l(\mathbf{t}') \geq f(\mathbf{t}') - \delta$. In particular, $\max_{l \in I_{\mathbf{t}}} p^l(\mathbf{t}') \geq f(\mathbf{t}') - \delta$ and thus $g(\mathbf{t}') \geq 0$. This allows to apply Lemma 2.3 and we receive

$$\min_{\mathbf{x}' \in [\mathbf{t}, \mathbf{t} + \Delta\mathbf{t}]} g(\mathbf{x}') \geq -\frac{3Ln}{n+1} \|\Delta\mathbf{t}\|_1.$$

Due to (2) it holds true that $\|\Delta\mathbf{t}\|_1 = \sum_{i=1}^n \Delta t_i \leq \frac{n+1}{n} \frac{\varepsilon - \delta}{3L}$. This then gives that for all $\mathbf{x} \in [\mathbf{t}, \mathbf{t} + \Delta\mathbf{t}]$, it is

$$\max_{l \in [K]} p^l(\mathbf{x}) - (f(\mathbf{x}) - \delta) \geq g(\mathbf{x}) \geq \min_{\mathbf{x}' \in [\mathbf{t}, \mathbf{t} + \Delta\mathbf{t}]} g(\mathbf{x}') \geq \delta - \varepsilon,$$

which is equivalent to

$$\max_{l \in [K]} p^l(\mathbf{x}) \geq f(\mathbf{x}) - \varepsilon.$$

Since \mathbf{t} was considered arbitrary and the domain \mathcal{D} is a union of all such boxes $[\mathbf{t}, \mathbf{t} + \Delta\mathbf{t}]$, the claim follows. \square

One can observe that the first condition (C1) is enforced by means of (5b) to (5d) together with the variables $s_{\mathbf{t}}^l$ and their integrality restriction. For (C2), the remaining constraints together with the non-negative variables $v_{\mathbf{d}}^l$ and the objective (5a) come into play.

Theorem 2.6 (Validity of (C2)). *If $(\alpha_i^l, \beta_i^l, \gamma^l)$, $v_{\mathbf{d}}^l$, for $\mathbf{d} \in \mathcal{G}$, $l \in [K]$, $i \in [n]$, satisfy the constraints (5e) to (5h) and have objective value (5a) of zero, then the paraboloids $(p^l)_{l \in [K]}$ defined by the parameters $(\alpha_i^l, \beta_i^l, \gamma^l)$ fulfill (C2).*

Proof. Recall from (4) that \mathcal{D} is the union of $[\mathbf{d}, \mathbf{d} + \Delta\mathbf{d}]$ over all $\mathbf{d} \in \mathcal{G} \cap [\mathbf{a}, \mathbf{b})$. Hence, consider an arbitrary but fixed $\mathbf{d} \in \mathcal{G} \cap [\mathbf{a}, \mathbf{b})$ and the box $[\mathbf{d}, \mathbf{d} + \Delta\mathbf{d}]$.

Observe that all vertices \mathbf{v} of this box are again vectors in \mathcal{G} . Therefore, constraints (5e) ensure that for all vertices \mathbf{v} and $l \in [K]$, it holds true that $p^l(\mathbf{v}) \leq f(\mathbf{v}) - \nu\varepsilon$.

Now, consider a fixed $l \in [K]$ and let $g(\mathbf{x}) := p^l(\mathbf{x}) - (f(\mathbf{x}) - \nu\varepsilon)$. Above gives $g(\mathbf{v}) \leq 0$ for all vertices \mathbf{v} of $[\mathbf{d}, \mathbf{d} + \Delta\mathbf{d}]$. In addition, by Lemma 2.2 and the constraints (5g) and (5h), p^l is Lipschitz with constant C . Using the triangle inequality we can show that g is Lipschitz continuous with constant $L_g = C + L$. By assumption the objective (5a) is zero and thus $v_{\mathbf{d}}^l = 0$. Combined with (5f) this implies $0 \geq \int_{[\mathbf{d}, \mathbf{d} + \Delta\mathbf{d}]} g(\mathbf{x}) d\mathbf{x}$. Therefore, we can apply Lemma 2.4 and receive

$$p^l(\mathbf{x}) - (f(\mathbf{x}) - \nu\varepsilon) = g(\mathbf{x}) \leq \max_{\mathbf{x}' \in [\mathbf{d}, \mathbf{d} + \Delta\mathbf{d}]} g(\mathbf{x}') \leq \frac{\sqrt{3}-1}{2} n(C+L) \max_{i \in [n]} \Delta d_i,$$

for all $\mathbf{x} \in [\mathbf{d}, \mathbf{d} + \Delta\mathbf{d}]$. From choosing Δd_i according to (3), we recall that $\Delta d_i \leq (2\nu\varepsilon)/((\sqrt{3}-1)n(C+L))$ and can conclude

$$p^l(\mathbf{x}) \leq f(\mathbf{x}).$$

Since $l \in [K]$ and \mathbf{d} were considered arbitrary and the domain \mathcal{D} is a union of all such boxes $[\mathbf{d}, \mathbf{d} + \Delta\mathbf{d}]$, the claim follows. \square

We have now established a model which is suitable to find an approximation with the desired conditions (C1) and (C2).

3. APPROXIMATION AND RELAXATION BY PARABOLOIDS

The previous MIP model is embedded in two search strategies to determine a small number of paraboloids for approximating a given function on a certain domain. Afterwards, we demonstrate ways to incorporate those approximations into MINLP problems and discuss potential benefits and drawbacks. If coupled with a relaxation of the general nonlinear constraints, we point out that the original MINLP is reduced to an Mixed-Integer Quadratically-Constrained Program (MIQCP). In a complementary step, we motivate creating a lookup table of approximations, which can be accessed when tackling MINLP problems by the parabolic relaxation.

3.1. Parabolic Approximation by Few Paraboloids. We start by recalling the setting: Let f be a Lipschitz continuous function with constant $L > 0$, which is to be approximated, and $\varepsilon > 0$ the desired approximation guarantee. Assume further that the choices of $\delta, \nu, C, \Delta t_i, \Delta d_i > 0$ comply with the requirements (2) and (3), as well as Theorem 2.1. The latter ensures the existence of a solution to problem (5) with $\bar{K} = |\mathcal{G}_\varepsilon|$, which meets the conditions (C1) and (C2).

Since each paraboloid results in an additional constraint when incorporated in the original problem later, we aim to find a small $K^* < \bar{K}$. A first idea is the application of a binary search in the discrete interval $[1, \bar{K}] =: [\underline{K}, \bar{K}]$. To this end, one starts by solving problem (5) with $K = \lfloor (\bar{K} + \underline{K})/2 \rfloor$. If an optimal solution with objective zero is returned, it defines a set of paraboloids which satisfy (C1) and (C2). Therefore, the upper bound is updated such that $\bar{K} \leftarrow K$. Otherwise, $\underline{K} \leftarrow K + 1$. After updating a bound, this procedure is restarted with respect to the new interval. It terminates when $\bar{K} \leq \underline{K}$ and returns $K^* \leftarrow \bar{K}$ as the minimal number of paraboloids. A formalization can be found in Algorithm 1.

However, since the initial \bar{K} is typically large, we propose a slight adjustment to the classical binary search. For a start, we set $K = 1$ and if the algorithm asserts in step 5, K is simply doubled in the next iteration, while respecting \bar{K} as an upper bound. This is performed, until the algorithm does not assert, i.e., until it detects a feasible number of paraboloids and updates the upper bound. Then, Algorithm 1 resumes as described and computes the minimal number of paraboloids K^* .

Algorithm 1 Number of Paraboloids – Binary Search

Input: an upper bound of paraboloids \bar{K}

Output: the minimal number of paraboloids K^* satisfying (C1) and (C2)

```

1: Set  $\underline{K} \leftarrow 1$ 
2: while  $\bar{K} > \underline{K}$  do
3:   Set  $K \leftarrow \lfloor (\bar{K} + \underline{K})/2 \rfloor$ 
4:   Solve (5) for  $K \rightarrow$  “infeasible” or objective  $c^K$ 
5:   if “infeasible” or  $c^K > 0$  then
6:     Set  $\underline{K} \leftarrow K + 1$ 
7:   else
8:     Set  $\bar{K} \leftarrow K$ 
9:   end if
10: end while
11: return  $K^* \leftarrow \bar{K}$ 

```

We note that the minimality of K^* is considered with respect to the MIP formulation (5). Indeed, there might exist an approximation with fewer paraboloids that satisfies the conditions (C1) and (C2), but is infeasible for (5). For instance, two of the paraboloids may not overlap at a predefined discretization point. In

addition, dependent on the particular form of f , an analytical solution may be computable by means of analytical and numerical methods.

It is also noteworthy that the size of problem (5) can increase to a non-negligible extend, especially when dealing with a large Lipschitz constant or a small accuracy. This effect is catalyzed when considering a large number of paraboloids K , as the entire problem size grows linearly in K . To deal with a potentially large problem size, we propose a second approach. It relaxes the original problem (5) by omitting constraints (5d) and determines the discretization widths Δt_i and Δd_i adaptively, not considering the assumptions (2) and (3). These measures decrease the problem size, but a solution may lack the desired conditions (C1) and (C2). Hence, we incorporate checks by solving small Nonlinear Programming (NLP) problems $\min_{\mathbf{x}}(f(\mathbf{x}) - \varepsilon - \max_l p^l(\mathbf{x}))$ and $\min_{\mathbf{x}}(\max_l p^l(\mathbf{x}) - f(\mathbf{x}))$ on the domain \mathcal{D} for a given $(p^l)_l$. This is achieved by remodeling to K inequalities or by solving K simpler problems, respectively. If the objectives are non-positive, the solution fulfills the desired property and we terminate. Otherwise, the number of paraboloids or the number of discretization points is increased and another loop is executed. We summarize this implementation in Algorithm 2.

Algorithm 2 Number of Paraboloids – Practical Implementation

Input: an upper bound of paraboloids \bar{K} , start values of discretization points $T_0, D_0 \in \mathbb{N}$ and paraboloids $K_0 < \bar{K}$

Output: a small number of paraboloids K^* satisfying (C1) and (C2)

```

1: Set  $T \leftarrow T_0, D \leftarrow D_0, K \leftarrow K_0$ 
2: while  $K < \bar{K}$  do
3:   Set  $T$ -bound  $\leftarrow$  false,  $D$ -bound  $\leftarrow$  false
4:   Compute  $\Delta t_i, \Delta d_i$  according to  $T, D$  for  $i \in [n]$ 
5:   Solve (5) without (5d)  $\rightarrow$  “infeasible” or solution  $(p^l)_{l \in [K]}$  with objective  $c^K$ 
6:   if “infeasible” or  $c^K > 0$  then
7:     Increment  $K$ 
8:   else
9:     Check (C2) by computing  $c^l := \min_{\mathbf{x} \in \mathcal{D}} \{p^l(\mathbf{x}) - f(\mathbf{x})\}$  for  $l \in [K]$ 
10:    if  $\exists l \in [K] : c^l > 0$  then
11:      Increase  $T$ 
12:    else
13:      Set  $T$ -bound  $\leftarrow$  true
14:    end if
15:    Shift each  $p^l$  by  $-c^l, l \in [K]$ 
16:    Check (C1) by computing  $c_\varepsilon := \min_{\mathbf{x} \in \mathcal{D}, y} \{y - (f(\mathbf{x}) - \varepsilon) \text{ s.t. } y \geq p^l(\mathbf{x}), l \in [K]\}$ 
17:    if  $c_\varepsilon < 0$  then
18:      Increase  $D$ 
19:    else
20:      Set  $D$ -bound  $\leftarrow$  true
21:    end if
22:  end if
23:  if  $T$ -bound and  $D$ -bound then
24:    Exit loop
25:  end if
26: end while
27: return  $K^* \leftarrow K$ 

```

3.2. Parabolic Relaxation. Turning to the original MINLP problem (1), we now assume to have a respective approximation $(p_j^l)_{l \in [K^j]}$ for each constraint function f_j . Then, we replace each f_j in (1) leading to

$$\begin{aligned} \min \quad & c(\mathbf{x}) \\ \text{s.t.} \quad & \max_{l \in [K^j]} p_j^l(\mathbf{x}) \leq y_j, & j \in J, \\ & \mathbf{x} \in \Omega. \end{aligned}$$

Since the maximum over all paraboloids is involved in a “ \leq ”-constraint, we equivalently reformulate this problem to

$$\min c(\mathbf{x}) \tag{6a}$$

$$\text{s.t. } p_j^l(\mathbf{x}) \leq y_j, \quad j \in J, l \in [K^j], \tag{6b}$$

$$\mathbf{x} \in \Omega. \tag{6c}$$

To the best of our knowledge, the only similar approach to this is performed in [20], where the authors use the minimum of paraboloids to compute a non-convex underestimator of a non-convex objective.

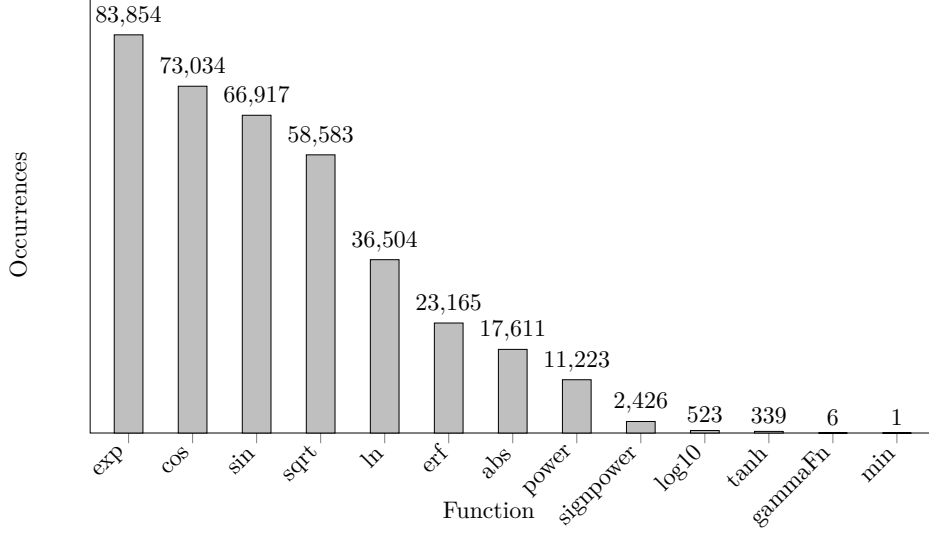
Since, without loss of generality, $c(\mathbf{x})$ can be assumed to be linear, this procedure creates a relaxation of the original MINLP to an MIQCP. In the realm of MINLP, exact solutions are typically out of scope and one is satisfied with an approximate solution with respect to some $\varepsilon > 0$. If a small enough approximation guarantee is considered when computing the approximations, solving the resulting MIQCP problem (6) returns a satisfactory solution for the original problem. This allows solvers tailored for MIQCP such as GloMIO [21] to be applied to an even broader problem class.

When solving such MIQCP problems, we emphasize that state-of-the-art solvers typically lift the problem to a higher dimension, in which quadratic functions are reduced to linear terms and simple squares, e.g., $\tilde{x} = x^2$. After the introduction of the first paraboloid p^1 each additional one p^l can therefore be considered as an additional linear constraint in the extended space. This allows to control the complexity of our approach, since tighter paraboloid relaxations can be realized by adding linear constraints. In the light of this, we propose to keep the general nonlinear constraints and to incorporate the parabolic constraints in addition.

Note that the representation of an MINLP like (1) is explicitly tailored for either strategy, but does not constitute a major limitation. For instance, assume that the right-hand side y_j is substituted by zero, resulting in a more general constraint $f_j(\mathbf{x}) \leq 0$. Then, two additional steps must be performed to apply the parabolic relaxation: First, one also requires an approximation of the hypograph of f_j , which can be obtained by executing the procedures in Section 3.1 for $-f_j$. Second, one introduces an auxiliary variables z_j , which serves as a replacement for f_j , leaving the original constraint $z_j \leq 0$, and bounds z_j from above and below by the computed approximations.

Now, going one step further, notice that most practical MINLP problems are *factorable*. This allows to represent each constraint function in terms of an *expression tree*, see, for instance, [25]. That is, each constraint function comprises of variables, constants, and nested elementary operations (such as ‘+’, ‘.’ or one-dimensional univariate functions). This can be depicted as an acyclic graph where every node is such a variable, constant, or operation, and this graph is called expression tree. By introduction of auxiliary variables a factorable MINLP problem can be transformed to only contain one-dimensional functions, as well as linear and bivariate terms. For an explanatory introduction of this procedure, see [22].

FIGURE 1. Cumulative occurrences of one dimensional function types in MINLPLib instances in OSIL-format



This representation is explicitly beneficial for the parabolic relaxation procedure because typically there already exists structures like $f_j(\mathbf{x}) = y_j$, where bounding y_j by paraboloids and relaxing this constraint is already sufficient. Hence, when referring to either strategy (replacement and addition) on a factorable MINLP, it is always assumed to apply this on suitable function components.

We like to highlight one potential pitfall for this procedure. The approximation guarantee for a one-dimensional component of an original constraint f_j might not propagate directly. The latter can worsen the overall accuracy and requires thorough analysis of the expression tree’s depth. We think of these aspects as accountable if respected.

3.3. Lookup Tables. To review our claim about factorability, we examine instances from the MINLPLib [10], a test set of various MINLP problems. Note that the majority of those instances is available in the OSIL-format, which is XML-based and mimics the expression tree. Thus, these instances are factorable.

This format also facilitates the analysis of the components of an instance. In Figure 1, we display the number of occurrences of one dimensional functions for all such instances. Hereby, occurrences of ‘power’ are not distinguished whether the exponent or the base is a variable or a constant. Further, the square function is excluded, since we argue to not approximate but keep those terms.

Observe that the exponential, the cosine, the sine, and the square root function occur very frequently. This allows to use a parabolic approximation to these functions repeatedly when tackling an entire subset of these problems. Naturally, the domain of their arguments varies dependent on the particular instance. However, an approximation for a wide domain is always valid for a subdomain. Therefore, we advocate to approximate these one dimensional functions with respect to some generic (e.g., the most common) domains and different approximation guarantees a-priori. The result serves as a lookup table for the parabolic relaxation.

The creation and usage of such a table can be interpreted as the common paradigm in the field of Machine Learning (ML). Once trained under potentially high computational effort, the ML approach is reused without significant cost in

every similar task. This applies for the lookup table and tackling a class of similar optimization problems with parabolic approximations.

At this point, it is important to note that a concatenation of approximations, i.e., sets of paraboloids, of two overlapping domains might not result in a globally valid one-sided approximation for the united domain. For instance, since the paraboloids are computed with respect to the original domain, one paraboloid can even intersect the function to approximate at a bound and leads to a violation of property (C2) right outside the domain.

Remark 3.1. *For the special case of the sine function, we highlight a potential enhancement of the procedure, which allows for concatenation. At first, one can find a parabolic approximation to the sine function from $-\pi/2$ to $3\pi/2$ and hereby restrict the sign of the quadratic coefficients to be non-positive. Then, we can observe that the approximation fulfills (C2) on \mathbb{R} entirely, as the paraboloids intersect somewhere below -1 at the bounds and decrease outside of the domain. At a second step, an approximation for an arbitrary (finite) domain can be computed by simply shifting the paraboloids appropriately and concatenating the solutions due to the periodicity of the sine. We even like to mention an approach by integer programming for unbounded domains for sine functions, where the integer variable keeps track of the period as an offset with respect to $[-\pi/2, 3\pi/2]$ and shifts the paraboloids accordingly. Naturally, both ideas can be applied analogously for the cosine function.*

4. COMPUTATIONAL RESULTS

We investigate the extend to which parabolic approximation and relaxation is sufficient for tackling MINLP problems in practice. To this end, we have implemented the MIP-based approaches for one-sided parabolic approximations discussed in Section 3.1 and analyze their ability to approximate functions (such as frequently occurring ones, see Figure 1) on different generic domains with varying accuracies. These results are used as a lookup table (compare Section 3.3) to apply the parabolic relaxation in two variants described in Section 3.2 to MINLPLib [10] instances.

All computational experiments are conducted on single nodes with Intel Xeon Gold 6326 “Ice Lake” multicore processors with 2.9GHz per core. The accessible RAM is set to 32 GB for the parabolic approximation and 64 GB for the parabolic relaxation with four and eight cores, respectively. All implementations are based on Python 3.11.7. The optimization problems are modeled via Pyomo [11, 17]. For the parabolic approximation, we solve the MIP models with Gurobi 11.0.3 [16] as a direct solver within Pyomo and leverage SCIP 8.1 as part of GAMS in version 46.4.0 for the checks. For the parabolic relaxation, we solve the resulting problems with Gurobi 11.0.1 and SCIP 8.1, both from inside the GAMS framework. If not stated otherwise, default settings are used. All code is available at <https://github.com/adriangoess/paraboloids.git> under a MIT license. The performance profiles for evaluation in Section 4.2 are created with the software [27].

4.1. Parabolic Approximation. To demonstrate the ability of our methods to approximate Lipschitz functions, we randomly generate a zigzag function as the first element for a test set. It is constructed by sampling uniformly and we refer to Appendix B.1 for details and the bold drawing in Figure 2 for an intuition. Further, since we aim to re-use the approximations computed here, we refer to Figure 1 and claim that an appropriate test set of functions is supposed to contain the exponential and the sine function. Approximations for \ln are assumed to require similar effort and for \cos they can be derived by scaling and translation. In order to additionally investigate the possibility of approximating higher order polynomials by parabolic (i.e., quadratic) terms, we include x^3 into the test set.

	domain \mathcal{D}					
zigzag	$[-5, -1]$	$[-2, 2]$	$[1, 5]$	$[-5, 0]$	$[0, -5]$	$[-5, 5]$
exp	$[-5, -2]$	$[-2, 2]$	$[-5, 2]$	$[2, 5]$	$[-2, 5]$	$[-5, 5]$
x^3	$[-2, 2]$	$[-5, 0]$	$[0, 5]$	$[-5, 2]$	$[-2, 5]$	$[-5, 5]$
sin	$[-\frac{\pi}{2}, \frac{\pi}{2}]$	$[\frac{\pi}{2}, \frac{3\pi}{2}]$	$[-\frac{\pi}{2}, \frac{3\pi}{2}]$	$[0, \pi]$	$[\pi, 2\pi]$	$[0, 2\pi]$

TABLE 1. Functions and domains to approximate by paraboloids.

Since we interpret the outcome discussed in this section as a lookup table, we take generic domains for each function into account. For zigzag, exp, and x^3 , we thus consider an interval of $[-5, 5]$ and several subintervals. For sin, we take the two periods $[-\pi/2, 3\pi/2]$ and $[0, 2\pi]$, as well as half of those into account, see Table 1 for an overview. Each function is approximated from above and below in order to highlight potential differences in the necessary number of paraboloids. For the approximation accuracy, we consider $\varepsilon \in \{10^0, 10^{-1}, 10^{-2}, 10^{-3}\}$.

For the zigzag function, we bound the interval for a uniform sample such that its Lipschitz constant is upper bounded by 1. This can always be enforced by scaling. Note that the Lipschitz constants for exp and x^3 can be computed as the maximal absolute derivative at the bounds. For instance, on $[-5, 2]$, this is $\exp(2)$ and $2(-5)^2$. For sin, we just consider the Lipschitz constant of 1, as this is the globally largest absolute derivative.

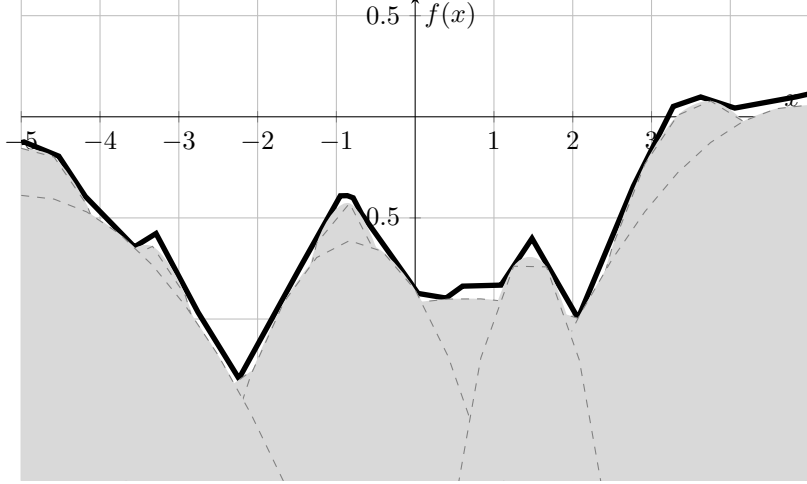
Recall that two methods for parabolic approximation have been presented in Section 3.1. One (**exact-MIP**) considers problem (5) unchanged and performs a binary search on the number of paraboloids, compare Algorithm 1. The other (**practical-MIP**) relaxes problem (5) to facilitate the solving process, but incorporates manual checks of conditions (C1) and (C2), see Algorithm 2 steps 9 and 16. These checks involve solving very small NLP problems, which we perform via SCIP.

Both methods require the specification of parameters to control the problem size. The method **exact-MIP** requires the definition of $\delta \in (0, \varepsilon)$ and $\nu \in (0, \delta/\varepsilon)$, which we set to $\varepsilon/2$ and $\delta/(2\varepsilon)$, respectively. Instead, for **practical-MIP**, the initial numbers of discretization points T_0 and D_0 need specification. Informally, the greater the Lipschitz constant, the wider the domain, or the smaller the accuracy, the more discretization points are required to satisfy the conditions. Translating these relations in a fractional term gives $T_0, D_0 \approx L|\mathcal{D}|/\varepsilon$. To keep the initial solution times low, we additionally divide by ten, resulting in $T_0 = D_0 = \lceil L|\mathcal{D}|/(10\varepsilon) \rceil$. For more details, we refer to the repository.

Based on these parameters, each method poses MIP problems which are solved using **Gurobi**. To maintain memory for the modeling, we set a limit of 24 GB from the available 32 GB for the solving process. In addition, the usable threads are limited to four and the solving time to 3600 s. Together with an iteration limit of 24, each run is theoretically bounded in time by 24 h, but typically falls short of it. We recall that when determining an initial feasible upper bound of paraboloids, the search number is doubled in every unsuccessful iteration. This can lead to a problem size that causes memory-based failures already in the modeling stage. To avoid such, we terminate whenever a problem shows more than 1,000 binary and 200,000 continuous variables and proceed with another iteration of the search respecting a smaller number.

Diving into the results, we start with the approximations of the zigzag function from below, see Table 2. Although having the theoretical guarantees as described in Section 2, the size of the corresponding MIP problems in **exact-MIP** for decreasing accuracy appears too large to be computationally tractable. Assuming the number

FIGURE 2. Approximation of the zigzag function from below by nine paraboloids with $\varepsilon = 10^{-1}$.



of paraboloids to be fixed, we note that when decreasing the accuracy by a factor of 10, in problem (5) the number of constraints grows by a factor of approximately 100 and the number of variables by 10. However, decreasing the accuracy by a certain factor intuitively results in a number of paraboloids increasing by a similar order of magnitude, which in turn enlarges the resulting problem even further. The adaption made for **practical-MIP** seems to cope with this increase to some extent, as it – in contrast – returns a result for the largest domain $[-5, 5]$ and $\varepsilon = 10^{-1}$ or for $[-5, -1]$ and $\varepsilon = 10^{-2}$. In Figure 2 we visualize the former result.

Interestingly, the number of paraboloids for the approximation is smaller with **practical-MIP**. This shows that the combination of constraints in problem (5) represents a sufficient condition for a global one-sided approximation, but not a necessary one. Since the results for the approximation from above are quite similar, we skip their explicit interpretation and refer to Table 12 in Appendix B.2.

\mathcal{D}	ε							
	10^0	10^{-1}	10^{-2}	10^{-3}	10^0	10^{-1}	10^{-2}	10^{-3}
$[-5, -1]$	2	5	-	-	1	4	41	-
$[-2, 2]$	2	9	-	-	1	4	-	-
$[-1, 5]$	2	7	-	-	1	4	-	-
$[-5, 0]$	2	8	-	-	1	5	-	-
$[0, 5]$	2	8	-	-	1	4	-	-
$[-5, 5]$	4	-	-	-	2	9	-	-
	exact-MIP				practical-MIP			

TABLE 2. Number of paraboloids to approximate the zigzag function from below.

Table 3 provides a summary for the results for **exp** approximated from above. Comparing the successful runs for either method, **practical-MIP** returns an approximation more frequently than **exact-MIP** and computes approximations relying on less paraboloids, which has already been observed for the zigzag function. However, either method struggles with the combination of a high accuracy and a large

\mathcal{D}	ε							
	10^0	10^{-1}	10^{-2}	10^{-3}	10^0	10^{-1}	10^{-2}	10^{-3}
$[-5, -2]$	1	1	3	-	1	1	2	5
$[-2, 2]$	3	-	-	-	2	5	32	-
$[-5, 2]$	4	-	-	-	3	8	81	-
$[2, 5]$	-	-	-	-	-	-	-	-
$[-2, 5]$	-	-	-	-	-	-	-	-
$[-5, 5]$	-	-	-	-	-	-	-	-
	exact-MIP				practical-MIP			

TABLE 3. Number of paraboloids to approximate exp from above.

\mathcal{D}	ε							
	10^0	10^{-1}	10^{-2}	10^{-3}	10^0	10^{-1}	10^{-2}	10^{-3}
$[-5, -2]$	1	1	3	-	1	1	2	8
$[-2, 2]$	3	-	-	-	2	4	20	-
$[-5, 2]$	3	-	-	-	2	6	56	-
$[2, 5]$	-	-	-	-	5	20	-	-
$[-2, 5]$	-	-	-	-	-	-	-	-
$[-5, 5]$	-	-	-	-	-	-	-	-
	exact-MIP				practical-MIP			

TABLE 4. Number of paraboloids to approximate exp from below.

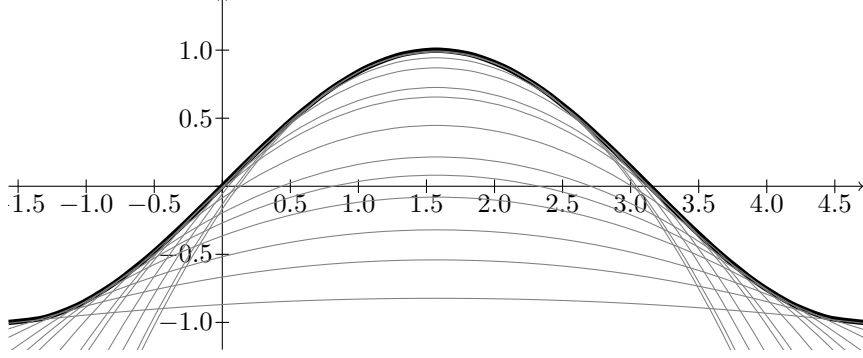
Lipschitz constant, both of which yield large MIP problems to solve. As noted above, the Lipschitz constant is computed as $\exp(\bar{x})$, where \bar{x} is the right bound of the domain. If $\bar{x} = 5$, the increase in the problem size causes the MIP problems to be intractable. This is also true for the approximations from below, see Table 4, except for cases with low accuracy on the smallest domain, which we account to the convexity of the epigraph of exp there. As the described effects are similar for approximating x^3 , we avoid further detailed discussion at this point and refer to Table 13 and Table 14 in Appendix B.3.

At first sight, these results seem to show tremendous limitations for parabolic approximations. But, one must recognize that the constructed MIP models basically rely on a Lipschitz property only and not on other properties like differentiability. This provides freedom to approximate general functions such as the zigzagging one, for instance, but is paid for with increased computational effort and thus limited success on specific functions.

Turning to the results for sin in Table 5 and Table 6, we remark a larger number of successful runs over all. The problem size seems to be controllable up to $\varepsilon = 10^{-1}$ for **exact-MIP** and $\varepsilon = 10^{-2}$ for **practical-MIP**. The latter approach is even successful for higher accuracy in some cases. In comparison to the zigzag function, for which the same Lipschitz constant of 1 is used, the methods are able to compute approximations more frequently. Beside the slightly smaller domain size, we assume that the regularity of sin facilitates finding adequate paraboloids, see Figure 3 for a visualization of this intuition.

In comparison to approximating exp or x^3 , we highlight the moderate number of paraboloids necessary for sin. This implies a small number of additional constraints

FIGURE 3. Approximation with $\varepsilon = 10^{-2}$ of \sin on $[-\pi/2, 3\pi/2]$ from below by 13 paraboloids.



\mathcal{D}	ε							
	10^0	10^{-1}	10^{-2}	10^{-3}	10^0	10^{-1}	10^{-2}	10^{-3}
$[-\pi/2, \pi/2]$	2	4	-	-	1	3	9	-
$[\pi/2, 3\pi/2]$	2	4	-	-	1	3	8	-
$[-\pi/2, 3\pi/2]$	3	9	-	-	1	5	47	-
$[0, \pi]$	1	3	-	-	1	1	5	40
$[\pi, 2\pi]$	1	2	-	-	1	1	3	32
$[0, 2\pi]$	3	7	-	-	2	5	24	-
	exact-MIP				practical-MIP			

TABLE 5. Number of paraboloids to approximate \sin from above.

\mathcal{D}	ε							
	10^0	10^{-1}	10^{-2}	10^{-3}	10^0	10^{-1}	10^{-2}	10^{-3}
$[-\pi/2, \pi/2]$	2	4	-	-	1	3	8	-
$[\pi/2, 3\pi/2]$	2	4	-	-	1	3	8	-
$[-\pi/2, 3\pi/2]$	2	5	-	-	1	3	13	-
$[0, \pi]$	1	2	-	-	1	1	3	16
$[\pi, 2\pi]$	1	3	-	-	1	1	5	-
$[0, 2\pi]$	3	7	-	-	2	5	44	-
	exact-MIP				practical-MIP			

TABLE 6. Number of paraboloids to approximate \sin from below.

when applying the parabolic relaxation to trigonometric functions. We analyze the resulting effects on a distinct set of instances in the following section.

4.2. Applied Parabolic Relaxation. To make use of the results above, we perform the parabolic relaxation on feasible instances from the MINLPLib [10] available in the OSIL-format. Due to this format, we can conveniently rewrite the instances as an expression tree in terms of quadratic parts and univariate functions such that we can identify parts to substitute, see Section 4.1. Since there exist results for approximation with $\varepsilon = 10^{-2}$ throughout the majority of relevant functions and domains, we fix this accuracy in the current section. For every instance, we

scan the expression tree formulation and identify a substitutable nonlinear function if its domain is a subset of the ones computed before and the domain width is nontrivial, i.e., $|\mathcal{D}| > 0$. We summarize all such instances as **all**. As discussed above, the substitution of \sin or \cos requires only a few paraboloids in comparison to \exp or x^3 . Therefore, we define the set **sub** as a filter on **all**, where we consider either instances with \sin and \cos , where there exist approximations for all nonlinear functions, or with \exp and x^3 , where there does not exist approximations for all nonlinear functions.

For each instance in the sets **all** and **sub**, we consider three types of problems: First, we take the instance in its original form into account, as given in GAMS-format on the MINLPLib website (**orig**). Second, we relax every possible one dimensional nonlinear function (**para**). For this, we follow the procedure described in Section 3.2. In particular, we reformulate each instance in terms of one-dimensional functions and linear/quadratic parts. This is complemented by an expression-tree-based bound propagation of the natural bounds of the respective arguments. Third, we keep the original functions and additionally incorporate the parabolic relaxation, aiming for the solvers to refine their relaxations with the quadratic cuts during the process (**both**). For details, we again refer to Section 3.2.

We tackle these problems with **Gurobi** and **SCIP**. Running on nodes with 64 GB of RAM, we limit the memory used by the solvers to 60 GB. Further, we apply a time limit of 4 h (14 400 s) and bound the usable threads by eight. Note that we experience numerical issues on one instance for each solver, which we exclude in the respective evaluation. An overview of all runs can be found in Table 15 in Appendix B.5, where we highlighted the excluded instance with an asterisk at the respective solver entry.

For comparison, we consider the optimality gap as a suitable metric. We leverage a definition that is widely used, e.g., by the solver CPLEX, and give it in absolute and relative terms. Formally, let c^* denote the best known value for (1) and d as a given lower/dual bound. The *absolute optimality gap* is then defined as

$$\text{absgap} = |c^* - d|,$$

and its relative analog as

$$\text{relgap} = |c^* - d| / (|c^*| + 10^{-10}) = \text{absgap} / (|c^*| + 10^{-10}).$$

This definition is independent of the presentation of (1) as a maximization or minimization problem. The addition of 10^{-10} avoids a division by zero. To keep the evaluation results for each solver independent of other solvers, we note that for each instance, c^* is defined as the best value among the one given on the MINLPLib website and the one returned by the current solver.

Since the results from Section 4.1 serve as an approximation with accuracy of $\varepsilon = 10^{-2}$, one cannot expect to have an optimality gap of zero on problems of type **para**. However, the method is expected to achieve comparable gaps with the returned dual value on a smaller time scale. Running **Gurobi** on **all** with type **orig** and **para**, see Table 7, we can unfortunately not observe such an effect. However, when executing **SCIP** on the same problems, we can see a significant decrease in the running times in the median, while maintaining comparable gaps, see Table 8. This effect even increases when restricting on **sub**, which has been declared before to be a more promising set of instances for the parabolic relaxation, see Table 9.

This motivates to dive deeper in the latter case. After removing all instances, on which **SCIP** requires less than 5 s on **orig** and **para**, Table 10 presents an overview of the remaining times and gaps. In the lower half, instances are gathered, on which the solver hits the time limit and returns comparable gaps for both problem types with one exception (**lnts400**). Turning to the instances in the upper half,

No. instances	orig		para	
	time in s	relgap	time in s	relgap
	38	38	38	38
Minimum	0.01	0.0000	0.01	0.0000
1st Quartile	0.08	0.0000	0.51	0.0024
Median	15.97	0.0001	102.07	0.0652
3rd Quartile	limit	0.5016	limit	0.5381
Maximum	limit	inf	limit	inf

TABLE 7. Statistics for Gurobi on **all**.

No. instances	orig		para	
	time in s	relgap	time in s	relgap
	38	38	38	38
Minimum	0.01	0.0000	0.01	0.0001
1st Quartile	0.49	0.0000	0.57	0.0049
Median	1774.99	0.0001	51.10	0.0389
3rd Quartile	limit	0.1405	limit	0.8334
Maximum	limit	6.5758	limit	inf

TABLE 8. Statistics for SCIP on **all**.

No. instances	orig		para	
	time in s	relgap	time in s	relgap
	23	23	23	23
Minimum	0.03	0.0000	0.04	0.0001
1st Quartile	0.39	0.0000	0.57	0.0116
Median	915.51	0.0001	25.70	0.0315
3rd Quartile	limit	0.0895	limit	0.5173
Maximum	limit	1.0000	limit	inf

TABLE 9. Statistics for SCIP on **sub**.

in all cases except the first, **SCIP** on type **para** requires a fraction of the solution time in comparison to **orig**. Except for instance t1000 the relative optimality gaps produced on the former is below 3.9%, which we consider quite small. Note that for t1000, the relative gap is high in comparison, but in absolute terms it is below 0.0001. This effect is caused by the optimal objective of zero and the corresponding division by a small term, compare the definition of relgap. Overall, these results are already promising and demonstrate the ability of **SCIP** to handle parabolic constraints efficiently.

This realization encourages to compare the performance of **SCIP** on **orig** and **both** types. Now, gaps of zero can be expected and, thus, a comparison in terms of sole running time is possible. This allows to use the metrics shifted geometric mean (SGM) of run time with a shift of 10 s [1] and performance profiles [27]. On instance set **all**, this results in a SGM of 530.6s for **orig** and 429.2s for **both**, where a virtual best of these types yields 379.3s. If we restrict the instance set to **sub**, the corresponding values are 535.6s, 319.3s, and 303.3s, respectively. This demonstrates that the instances equipped with parabolic approximations on top

instance	orig		para	
	run time in s	relgap	run time in s	relgap
ghg_1veh	19.44	0.0001	25.70	0.0003
pooling_epa1	53.93	0.0001	9.42	0.0389
kriging[...].red020	773.66	0.0001	19.23	0.0224
t1000	915.51	0.0000	0.57	0.9990
lnts50	limit	0.0258	51.10	0.0228
pooling_epa2	limit	0.0151	2047.92	0.0151
lnts100	limit	0.0345	3889.47	0.0315
contvar	limit	0.5024	limit	0.5031
ex8_4_6	limit	1.0000	limit	1.0000
feedtray	limit	0.8048	limit	0.5762
ghg_2veh	limit	0.0447	limit	0.0426
ghg_3veh	limit	0.5200	limit	0.5173
lnts200	limit	0.0895	limit	0.0864
lnts400	limit	0.1153	limit	inf
pooling_epa3	limit	0.0041	limit	0.0309

TABLE 10. SCIP on sub with run time > 5 s.

of the original constraints are solved faster on average. In particular, the solving times are reduced by more than 40% when applied to an instance class, which can be identified a-priori.

The acceleration of SCIP by our approach is confirmed when looking at the performances profiles in Figure 4 for all. A certain price in terms of time is paid due to the overhead of additional parabolic constraints on instances, which are originally solved fast. However, SCIP seems to leverage the paraboloids for the other instances in order to boost the solving process significantly. This effect is even enhanced when tackling the promising instances sub, see Figure 5.

In general, the computations indicate a huge potential to accelerate the solving process of MINLP problems by means of paraboloids. In Section 3.2, we have laid out how additional parabolic constraints do not increase the complexity of the underlying problem. This suggests to interpret parabolic constraints as quadratic cuts. Now, when solving MIP problems in practice, a solver does not incorporate all potential cuts at the root node, but applies them to strengthen the continuous relaxation adaptively throughout the branch-and-bound scheme. Consequently, in MINLP, we strongly believe that there is still room for improvement of this approach by integrating the parabolic cuts into a spatial branch-and-bound framework, since it keeps intermediate problem sizes low while providing tight relaxations selectively.

5. CONCLUSION & FUTURE WORK

We proposed a quadratic approximation approach for solving general Mixed-Integer Nonlinear Programming (MINLP) problems. Our method globally approximates nonlinear constraint functions with paraboloids and directly incorporates the resulting parabolic constraints into the original MINLP formulation. To construct these approximations, we combined tailored search methods with a Mixed-Integer Linear Programming (MIP) model, for which we provide theoretical verification. Moreover, we presented two main strategies for effectively integrating these approximations into MINLP models. We tested both strategies - approximation and incorporation - computationally on common functions and several instances from the MINLPlib, respectively, demonstrating promising numerical results.

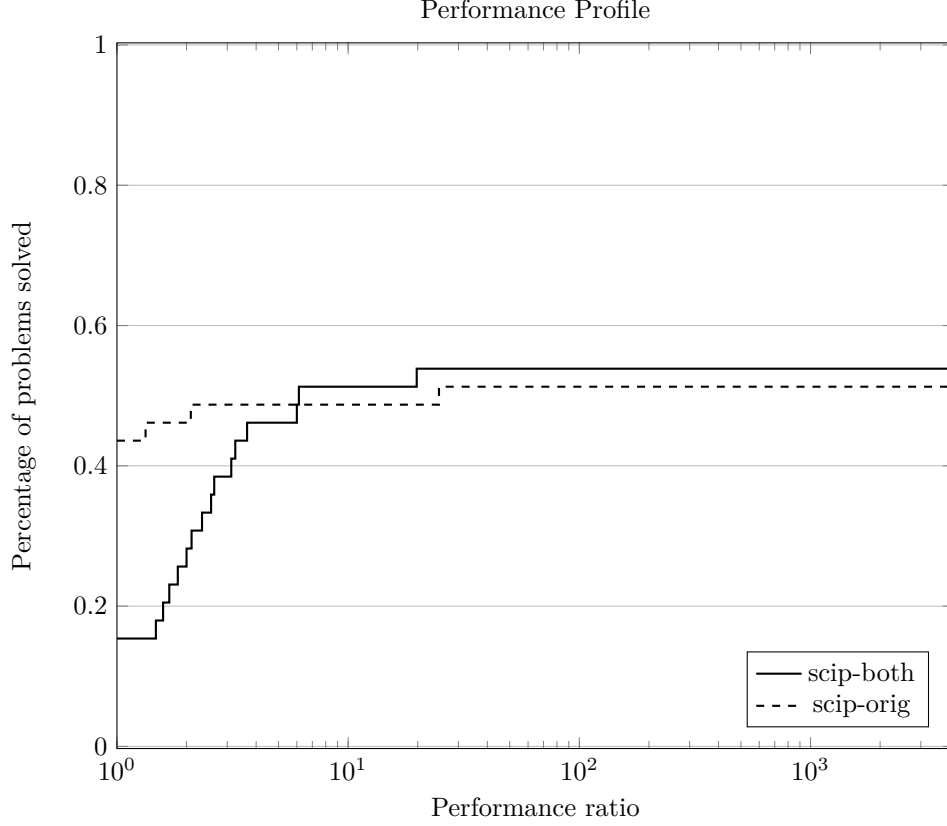


FIGURE 4. SCIP on all with orig and both.

We see significant potential in combining our parabolic approximation approach with established optimization techniques. In fact, adaptively incorporating parabolic constraints can be interpreted as a nonlinear counterpart to linear cutting-plane methods such as Gomory cuts. Hence, it appears particularly promising to embed our approach within spatial branch-and-bound frameworks, enabling concatenation of approximation results, domain splitting, and adaptive refinement of quadratic approximations. Moreover, combining parabolic approximations with adaptive cutting methods could further tighten relaxations, reduce initial problem sizes, and yield improved dual bounds.

Although our experiments showed clear improvements and practical benefits, the approximation scheme still offers room for enhancement. Considering the analysis of expression trees, we suggest specializing the approximation scheme for one-dimensional functions by leveraging additional structural properties, such as differentiability. Such targeted approximations would allow tackling larger domains and enable smaller accuracies, potentially further improving computational performance. In conclusion, our method provides a flexible and complementary tool for MINLP problems and suggests several promising directions for future research.

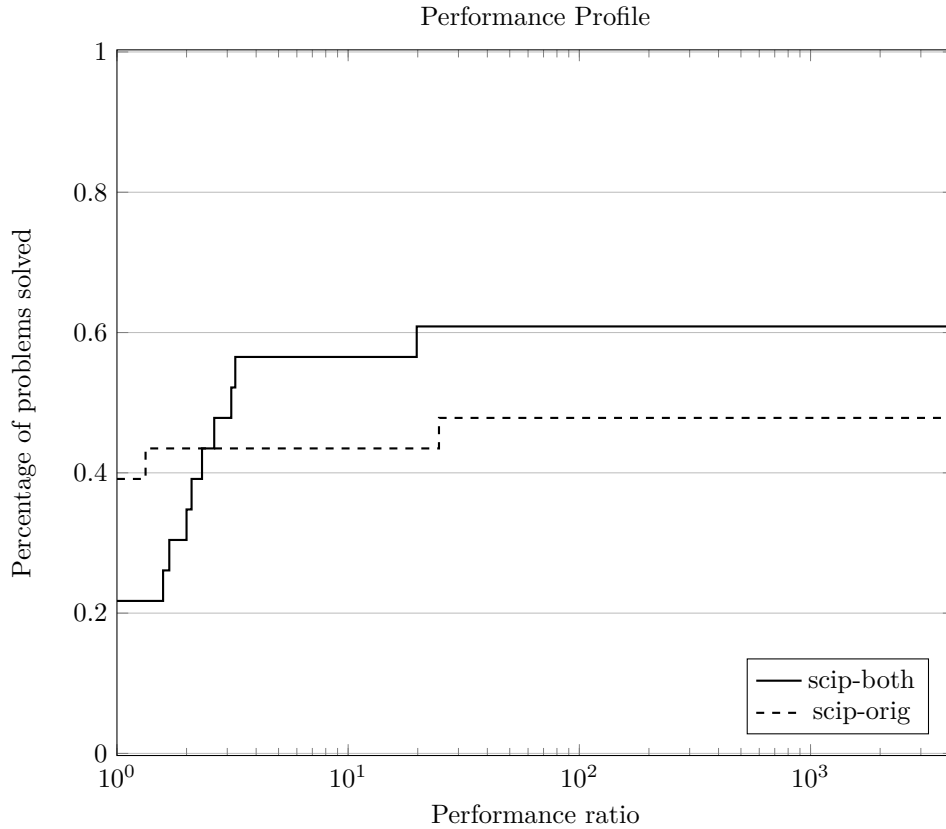


FIGURE 5. SCIP on sub with orig and both.

REFERENCES

- [1] T. Achterberg. “Constraint integer programming.” PhD thesis. 2007.
- [2] J. H. Ahlberg, E. N. Nilson, and J. L. Walsh. *The Theory of Splines and Their Applications: Mathematics in Science and Engineering: A Series of Monographs and Textbooks*. Vol. 38. Elsevier, 2016.
- [3] I. P. Androulakis, C. D. Maranas, and C. A. Floudas. “ α BB: A global optimization method for general constrained nonconvex problems.” In: *Journal of Global Optimization* 7.4 (Dec. 1, 1995), pp. 337–363. DOI: [10.1007/BF01099647](https://doi.org/10.1007/BF01099647). URL: <https://doi.org/10.1007/BF01099647>.
- [4] B. Beach, R. Burlacu, A. Bärmann, L. Hager, and R. Hildebrand. “Enhancements of discretization approaches for non-convex mixed-integer quadratically constrained quadratic programming: Part I.” In: *Computational Optimization and Applications* 87.3 (Apr. 1, 2024), pp. 835–891. DOI: [10.1007/s10589-023-00543-7](https://doi.org/10.1007/s10589-023-00543-7). URL: <https://doi.org/10.1007/s10589-023-00543-7>.
- [5] B. Beach, R. Hildebrand, and J. Huchette. “Compact mixed-integer programming formulations in quadratic optimization.” In: *Journal of Global Optimization* 84.4 (2022), pp. 869–912.
- [6] P. Belotti, C. Kirches, S. Leyffer, J. Linderoth, J. Luedtke, and A. Mahajan. “Mixed-integer nonlinear optimization.” In: *Acta Numerica* 22 (2013), pp. 1–131. DOI: [10.1017/S0962492913000032](https://doi.org/10.1017/S0962492913000032).
- [7] R. Bojanic and R. DeVore. “On polynomials of best one-sided approximation.” In: *Enseign. Math* 12 (1966), pp. 139–164.

- [8] L. Buchheim Christoph and Trieu. “Quadratic Outer Approximation for Convex Integer Programming with Box Constraints.” In: *Experimental Algorithms*. Ed. by C. Bonifaci Vincenzo and Demetrescu and A. Marchetti-Spaccamela. Berlin, Heidelberg: Springer Berlin Heidelberg, 2013, pp. 224–235.
- [9] R. Burlacu. “Adaptive mixed-integer refinements for solving nonlinear problems with discrete decisions.” PhD thesis. 2020.
- [10] M. R. Bussieck, A. S. Drud, and A. Meeraus. “MINLPLib—a collection of test models for mixed-integer nonlinear programming.” In: *INFORMS Journal on Computing* 15.1 (2003), pp. 114–119.
- [11] M. L. Bynum, G. A. Hackebeit, W. E. Hart, C. D. Laird, B. L. Nicholson, J. D. Siirola, J.-P. Watson, and D. L. Woodruff. *Pyomo—optimization modeling in python*. Third. Vol. 67. Springer Science & Business Media, 2021.
- [12] M. V. Deikalova and A. Y. Torgashova. “Best One-Sided Approximation in the Mean of the Characteristic Function of an Interval by Algebraic Polynomials.” In: *Proceedings of the Steklov Institute of Mathematics* 308.1 (Apr. 1, 2020), pp. 68–82. DOI: [10.1134/S0081543820020066](https://doi.org/10.1134/S0081543820020066). URL: <https://doi.org/10.1134/S0081543820020066>.
- [13] M. A. Duran and I. E. Grossmann. “An outer-approximation algorithm for a class of mixed-integer nonlinear programs.” In: *Mathematical programming* 36.3 (1986), pp. 307–339.
- [14] B. Geißler, A. Martin, A. Morsi, and L. Schewe. “Using Piecewise Linear Functions for Solving MINLPs.” In: *Mixed Integer Nonlinear Programming*. Ed. by J. Lee and S. Leyffer. New York, NY: Springer New York, 2012, pp. 287–314.
- [15] A. M. Geoffrion. “Generalized benders decomposition.” In: *Journal of optimization theory and applications* 10.4 (1972), pp. 237–260.
- [16] Gurobi Optimization, LLC. *Gurobi Optimizer Reference Manual, Version 11.0*. 2023. URL: <https://www.gurobi.com>.
- [17] W. E. Hart, J.-P. Watson, and D. L. Woodruff. “Pyomo: modeling and solving mathematical programs in Python.” In: *Mathematical Programming Computation* 3.3 (2011), pp. 219–260.
- [18] R. Horst and H. Tuy. *Global optimization: Deterministic approaches*. Third. Springer Science & Business Media, 1996.
- [19] J. T. Lewis. “Computation of best one-sided L_1 approximation.” In: *Mathematics of Computation* 24.111 (1970), pp. 529–536.
- [20] O. L. Mangasarian, J. B. Rosen, and M. E. Thompson. “Nonconvex Piecewise-Quadratic Underestimation for Global Minimization.” In: *Journal of Global Optimization* 34.4 (2006), pp. 475–488.
- [21] R. Misener and C. A. Floudas. “GloMIQO: Global mixed-integer quadratic optimizer.” In: *Journal of Global Optimization* 57.1 (Sept. 1, 2013), pp. 3–50. DOI: [10.1007/s10898-012-9874-7](https://doi.org/10.1007/s10898-012-9874-7). URL: <https://doi.org/10.1007/s10898-012-9874-7>.
- [22] A. Morsi. “Solving MINLPs on Loosely-coupled Networks with Applications in Water and Gas Network Optimization.” PhD thesis. 2013.
- [23] G. Nürnberger. *Approximation by spline functions*. Vol. 1. Springer, 1989.
- [24] H. S. Ryoo and N. V. Sahinidis. “A branch-and-reduce approach to global optimization.” In: *Journal of Global Optimization* 8.2 (Mar. 1, 1996), pp. 107–138. DOI: [10.1007/BF00138689](https://doi.org/10.1007/BF00138689). URL: <https://doi.org/10.1007/BF00138689>.
- [25] H. Schichl and A. Neumaier. “Interval Analysis on Directed Acyclic Graphs for Global Optimization.” In: *Journal of Global Optimization* 33.4 (Dec. 1, 2005), pp. 541–562. DOI: [10.1007/s10898-005-0937-x](https://doi.org/10.1007/s10898-005-0937-x). URL: <https://doi.org/10.1007/s10898-005-0937-x>.

- [26] L. Schumaker. *Spline functions: basic theory*. Cambridge university press, 2007.
- [27] A. S. Siqueira, R. G. C. da Silva, and L.-R. Santos. “Perprof-py: A python package for performance profile of mathematical optimization software.” In: *Journal of Open Research Software* 4.1 (2016), e12–e12.
- [28] M. Tawarmalani and N. V. Sahinidis. *Convexification and global optimization in continuous and mixed-integer nonlinear programming: theory, algorithms, software, and applications*. Vol. 65. Springer Science & Business Media, 2013.
- [29] J. P. Vielma. “Mixed Integer Linear Programming Formulation Techniques.” In: *SIAM Review* 57.1 (2015), pp. 3–57. DOI: [10.1137/130915303](https://doi.org/10.1137/130915303). eprint: <https://doi.org/10.1137/130915303>. URL: <https://doi.org/10.1137/130915303>.
- [30] T. Westerlund and F. Pettersson. “An extended cutting plane method for solving convex MINLP problems.” In: *Computers & chemical engineering* 19 (1995), pp. 131–136.
- [31] S. Wiese. *A computational practicability study of MIQCQP reformulations*. 2021. URL: <https://docs.mosek.com/whitepapers/miqcqp.pdf> (visited on 06/17/2024).

APPENDIX A. PROOFS FOR LEMMATA IN SECTION 2

A.1. Proof of Theorem 2.1.

Proof. We want to prove the statement constructively. In particular, for every $\mathbf{t} \in \mathcal{G}_\varepsilon$, we define an explicit paraboloid p such that all of these paraboloids fulfill the constraints of problem (5). As the grid widths are chosen identically, we can interchange $\mathbf{t} \in \mathcal{G}_\varepsilon$ and $\mathbf{d} \in \mathcal{G}$.

First, see that

$$\sum_{i=1}^n \Delta t_i = n\Delta \leq \frac{n+1}{n} \frac{\varepsilon - \delta}{3L}.$$

Hence, the choice of Δt_i is in accordance with the required property (2). The property (3) follows by construction.

Now, consider an arbitrary but fixed vector $\mathbf{t} \in \mathcal{G}_\varepsilon$. Then, the vertices \mathbf{v} of $[\mathbf{t} - \Delta, \mathbf{t} + \Delta]$ are exactly the elements in $\mathcal{N}(\mathbf{t})$. This allows for a parameterized representation of the vertices as $\mathbf{v}_\mathbf{u} := \mathbf{t} + \Delta \sum_{i=1}^n u_i \mathbf{e}_i$ for all $\mathbf{u} \in \{-1, 1\}^n$, where \mathbf{e}_i denotes the i th unit vector.

Notice that a paraboloid $p(\mathbf{x}) = \sum_{i=1}^n \alpha_i x_i^2 + \beta_i x_i + \gamma$ has $2n + 1$ coefficients. Hence, it is uniquely determined by solving the following system of equations:

$$p(\mathbf{t}) = f(\mathbf{t}) - \delta, \tag{7}$$

$$\frac{d}{dx_i} p(\mathbf{v}_\mathbf{u}) = -u_i 2L, \quad \text{for all } \mathbf{u} \in \{-1, 1\}^n, i \in [n]. \tag{8}$$

The 2^n many equations (8) can be rewritten as the system

$$2\alpha_i(t_i + \Delta) + \beta_i = -2L \quad \wedge \quad 2\alpha_i(t_i - \Delta) + \beta_i = 2L, \tag{9}$$

for all $i \in [n]$, which has $2n$ equations. Solving (9), we receive $\alpha_i = -L/\Delta$ and $\beta_i = 2Lt_i/\Delta$. As γ is the only degree of freedom left, we compute it by solving (7). Therefore, such a p exists and is uniquely determined. As p fulfills equation (7) for \mathbf{t} , we can set $s_\mathbf{t} = 1$ for this p and, thus, with (8), our construction satisfies (5b)-(5d).

In order to prove conformity with constraints (5e) and (5f), we abstract the situation and assume $\mathbf{t} = \mathbf{d} = \mathbf{0}$. Following the computations from before, it is $\gamma = f(\mathbf{0}) - \delta$, $\alpha_i = -L/\Delta$ and $\beta_i = 0$. Now, if we show

$$f(\mathbf{x}) - \nu\varepsilon - p(\mathbf{x}) \geq 0, \text{ for all } \mathbf{x} \in [-\Delta, \Delta], \tag{10}$$

this transfers to the original box $[\mathbf{d} - \Delta, \mathbf{d} + \Delta]$ and directly gives (5e). Furthermore, inequality (10) implies that the argument of the integral in (5f) is non-positive, which implies $v_\mathbf{d} = 0$ if combined with the objective function.

To show (10), we remark that the Lipschitz continuity of f at a point \mathbf{x} gives $f(\mathbf{x}) \geq f(\mathbf{0}) - L\|\mathbf{x}\|_1 =: \Lambda(\mathbf{x})$. Then, the (sub)gradient $\nabla \Lambda(\mathbf{x}) = -L \operatorname{sgn}(\mathbf{x})$, where $\operatorname{sgn}(\mathbf{x})$ is the component-wise sign function. Now, defining the auxiliary function $g(\mathbf{x}) := \Lambda(\mathbf{x}) - \nu\varepsilon - p(\mathbf{x})$, we want to show $\min_{\mathbf{x}} g(\mathbf{x}) \geq 0$. From (7), we derive

$$g(\mathbf{0}) = \Lambda(\mathbf{0}) - \nu\varepsilon - p(\mathbf{0}) = f(\mathbf{0}) - \delta/2 - f(\mathbf{0}) + \delta > 0.$$

As $\alpha_i < 0$, it also holds true that

$$\lim_{\|\mathbf{x}\|_1 \rightarrow \infty} g(\mathbf{x}) = \lim_{\|\mathbf{x}\|_1 \rightarrow \infty} f(\mathbf{0}) - L\|\mathbf{x}\|_1 - \nu\varepsilon - p(\mathbf{x}) = \infty.$$

Hence, suitable candidates for achieving $\min_{\mathbf{x}} g(\mathbf{x})$ must fulfill $\nabla g(\mathbf{x}) = \mathbf{0}$, which gives

$$\mathbf{0} = \nabla g(\mathbf{x}) = -L \operatorname{sgn}(\mathbf{x}) + (2L/\Delta)\mathbf{x}.$$

For a solution \mathbf{x}' to this equation, it holds true that $x'_i = \pm\Delta/2$ for $i \in [n]$. Evaluating p with the coefficients computed before at \mathbf{x}' gives

$$p(\mathbf{x}') = \sum_{i=1}^n (-L/\Delta)(\Delta/2)^2 + f(\mathbf{0}) - \delta = -nL\Delta/4 + f(\mathbf{0}) - \delta.$$

The respective value of g is

$$\begin{aligned} g(\mathbf{x}') &= f(\mathbf{0}) - L\|\mathbf{x}'\|_1 - \nu\varepsilon - p(\mathbf{x}') \\ &= f(\mathbf{0}) - Ln\Delta/2 - \nu\varepsilon + nL\Delta/4 - f(\mathbf{0}) + \delta \\ &= \delta/2 - nL\Delta/4 \geq \delta/2 - nL\delta/(2nL) = 0, \end{aligned}$$

using the choice $\nu = \delta/(2\varepsilon)$ and $\Delta \leq (2\delta)/(nL)$. In summary, this shows that $\min_{\mathbf{x}} g(\mathbf{x}) \geq 0$ and thus

$$f(\mathbf{x}) - \nu\varepsilon - p(\mathbf{x}) \geq \Lambda(\mathbf{x}) - \nu\varepsilon - p(\mathbf{x}) = g(\mathbf{x}) \geq \min_{\mathbf{x}} g(\mathbf{x}) \geq 0.$$

In particular, (5e) is true for p , as well as (5f) for $v_{\mathbf{d}} = 0$, $\mathbf{d} \in \mathcal{G}$.

Lastly, we prove the feasibility of p for constraints (5g) and (5h). From above, we have the explicit representation of α_i and β_i , $i \in [n]$. Hence, we directly derive

$$\begin{aligned} \left| \frac{d}{dx_i} p(\mathbf{a}) \right| &= |2\alpha_i a_i + \beta_i| = |-2La_i/\Delta + 2Lt_i/\Delta| = \frac{2L}{\Delta} |t_i - a_i| \\ &= \frac{2L}{\Delta} (t_i - a_i) \leq \frac{2L}{\Delta} (b_i - a_i) \leq \frac{2L}{\Delta} \|\mathbf{b} - \mathbf{a}\|_{\infty} = C. \end{aligned}$$

This shows that p satisfies (5g). The case for (5h) follows analogously. This concludes the proof. \square

A.2. Proof of Lemma 2.2.

Proof. Let $i \in [n]$ be arbitrary but fixed. Note that $\frac{d}{dx_i} p(\mathbf{x}) = 2\alpha_i x_i + \beta_i$. This is a linear term in x_i . Since $\mathbf{x} \in \mathcal{D}'$, it is $a'_i \leq x_i \leq b'_i$. Hence, the bounds on the absolute derivative at \mathbf{a}' and \mathbf{b}' are equivalent to bounding a linear term in absolute values between a'_i and b'_i . So, the first claim about the general bound of the derivative on \mathcal{D}' follows.

Now, let $\mathbf{x}, \mathbf{y} \in \mathcal{D}'$, and $g(\lambda) := p((1-\lambda)\mathbf{x} + \lambda\mathbf{y})$. By the chain rule, it follows that $g'(\lambda) = \frac{d}{d\lambda} g(\lambda) = \nabla p((1-\lambda)\mathbf{x} + \lambda\mathbf{y})^\top (\mathbf{y} - \mathbf{x})$. By the mean value theorem, there exists $\hat{\lambda} \in [0, 1]$ such that

$$g(1) - g(0) = g'(\hat{\lambda})(1 - 0) = g'(\hat{\lambda}),$$

and it follows

$$|p(\mathbf{x}) - p(\mathbf{y})| = |g(1) - g(0)| = |g'(\hat{\lambda})| = |\nabla p((1-\hat{\lambda})\mathbf{x} + \hat{\lambda}\mathbf{y})^\top (\mathbf{y} - \mathbf{x})|.$$

In order to show the Lipschitz continuity of p , we now have to find a bound for the upper. This is achieved by an application of Hölder's inequality, in particular,

$$|p(\mathbf{x}) - p(\mathbf{y})| \leq \|\nabla p((1-\hat{\lambda})\mathbf{x} + \hat{\lambda}\mathbf{y})\|_1 \|\mathbf{y} - \mathbf{x}\|_{\infty} \leq nC \|\mathbf{y} - \mathbf{x}\|_{\infty},$$

and

$$|p(\mathbf{x}) - p(\mathbf{y})| \leq \|\nabla p((1-\hat{\lambda})\mathbf{x} + \hat{\lambda}\mathbf{y})\|_{\infty} \|\mathbf{y} - \mathbf{x}\|_1 \leq C \|\mathbf{y} - \mathbf{x}\|_1,$$

respectively, where we used the bounded partial derivative in each last step. This shows the second claim. \square

A.3. Proof of Lemma 2.3.

Proof. Let $g^* := g(\mathbf{x}^*) := \min_{\mathbf{x} \in \mathcal{D}'} g(\mathbf{x})$. Note that g^* is finite, since g is (Lipschitz) continuous and \mathcal{D}' is compact. Hence, the point $\mathbf{x}^* \in \mathcal{D}'$ exists.

Now, by Caratheodory's Theorem, there exist vertices $\mathbf{v}^1, \dots, \mathbf{v}^{n+1}$ of \mathcal{D}' such that

$$\mathbf{x}^* = \sum_{j=1}^{n+1} \lambda_j \mathbf{v}^j \quad \wedge \quad \sum_{j=1}^{n+1} \lambda_j = 1 \quad \wedge \quad \lambda_j \geq 0, \text{ for all } j \in [n+1].$$

Next, let $k \in [n+1]$. Then, we can rewrite the first equality from above to

$$\mathbf{x}^* - \mathbf{v}^k = \sum_{\substack{j=1, \\ j \neq k}}^{n+1} \lambda_j \mathbf{v}^j + (\lambda_k - 1) \mathbf{v}^k = \sum_{\substack{j=1, \\ j \neq k}}^{n+1} \lambda_j \mathbf{v}^j - \sum_{\substack{j=1, \\ j \neq k}}^{n+1} \lambda_j \mathbf{v}^k = \sum_{j=1}^{n+1} \lambda_j (\mathbf{v}^j - \mathbf{v}^k),$$

where we used that the sum of λ_j is one in the second and $\mathbf{v}^k - \mathbf{v}^k = \mathbf{0}$ in the last step.

By leveraging $g(\mathbf{v}^k) \geq 0$ from the assumption, the minimality of $g(\mathbf{x}^*)$, and the Lipschitz continuity of g (in this order), we derive

$$\begin{aligned} -g(\mathbf{x}^*) &= 0 - g(\mathbf{x}^*) \leq g(\mathbf{v}^k) - g(\mathbf{x}^*) = |g(\mathbf{v}^k) - g(\mathbf{x}^*)| \leq L_g \|\mathbf{v}^k - \mathbf{x}^*\|_1 \\ &= L_g \left\| \sum_{j=1, j \neq k}^{n+1} \lambda_j (\mathbf{v}^j - \mathbf{v}^k) \right\|_1 = L_g \sum_{i=1}^n \left| \sum_{j=1}^{n+1} \lambda_j (v_i^j - v_i^k) \right|. \end{aligned}$$

Note that the i th entry of any vertex \mathbf{v} is either a'_i or b'_i . This implies that the inner bracket is non-negative if $v_i^k = a'_i$ and non-positive if $v_i^k = b'_i$. Having this in mind and rearranging the sums, we can further rewrite the right-hand side of the upper inequality as

$$\begin{aligned} L_g \sum_{i \in [n]} \left| \sum_{j=1}^{n+1} \lambda_j (v_i^j - v_i^k) \right| &= L_g \left[\sum_{\substack{i \in [n], \\ v_i^k = a'_i}} \sum_{j=1}^{n+1} \lambda_j (v_i^j - v_i^k) + \sum_{\substack{i \in [n], \\ v_i^k = b'_i}} \sum_{j=1}^{n+1} \lambda_j (v_i^k - v_i^j) \right] \\ &= L_g \left[\sum_{j=1}^{n+1} \lambda_j \sum_{\substack{i \in [n], \\ v_i^k = a'_i}} (v_i^j - v_i^k) + \sum_{j=1}^{n+1} \lambda_j \sum_{\substack{i \in [n], \\ v_i^k = b'_i}} (v_i^k - v_i^j) \right] \\ &= L_g \sum_{j=1}^{n+1} \lambda_j \sum_{\substack{i \in [n], \\ v_i^k \neq v_i^j}} (b'_i - a'_i). \end{aligned}$$

Here, $\lambda_j \geq 0$ allows to omit the absolute value in the first equality and one needs to note that the inner brackets are $b'_i - a'_i$ if and only if $v_i^k \neq v_i^j$. In conclusion, we receive

$$-g(\mathbf{x}^*) \leq L_g \sum_{j=1}^{n+1} \lambda_j \sum_{\substack{i \in [n], \\ v_i^k \neq v_i^j}} (b'_i - a'_i).$$

Summing this over k gives

$$-(n+1)g(\mathbf{x}^*) \leq L_g \sum_{k=1}^{n+1} \sum_{j=1}^{n+1} \lambda_j \sum_{\substack{i \in [n], \\ v_i^k \neq v_i^j}} (b'_i - a'_i) = L_g \sum_{j=1}^{n+1} \lambda_j \sum_{k=1}^{n+1} \sum_{\substack{i \in [n], \\ v_i^k \neq v_i^j}} (b'_i - a'_i)$$

$$\begin{aligned}
&= L_g \sum_{j=1}^{n+1} \lambda_j \sum_{\substack{k=1, \\ k \neq j}}^{n+1} \sum_{\substack{i \in [n], \\ v_i^k \neq v_i^j}} (b'_i - a'_i) \leq L_g \sum_{j=1}^{n+1} \lambda_j n \sum_{i=1}^n (b'_i - a'_i) \\
&= L_g n \sum_{j=1}^{n+1} \lambda_j \|\mathbf{b}' - \mathbf{a}'\|_1 = L_g n \|\mathbf{b}' - \mathbf{a}'\|_1.
\end{aligned}$$

A division by $-(n+1)$ then gives the desired bound and finishes the proof. \square

A.4. Proof of Lemma 2.4.

Proof. Let $g^* := g(\mathbf{x}^*) := \max_{\mathbf{x} \in \mathcal{D}'} g(\mathbf{x})$. Again, note that g^* is finite and such a point \mathbf{x}^* exists due to the (Lipschitz) continuity of g and the compactness of \mathcal{D}' .

Since g is Lipschitz, we have

$$g^* - g(\mathbf{x}) = |g(\mathbf{x}^*) - g(\mathbf{x})| \leq L_g \|\mathbf{x} - \mathbf{x}^*\|_1,$$

which is equivalent to

$$g(\mathbf{x}) \geq g^* - L_g \|\mathbf{x} - \mathbf{x}^*\|_1 =: \Lambda(\mathbf{x}), \quad (11)$$

for all $\mathbf{x} \in \mathcal{D}'$. Now, with the assumption and by writing $V := \text{vol}(\mathcal{D}')$, we derive

$$\begin{aligned}
0 &\geq \int_{\mathcal{D}'} g(\mathbf{x}) d\mathbf{x} \geq \int_{\mathcal{D}'} \Lambda(\mathbf{x}) d\mathbf{x} = \int_{\mathcal{D}'} g^* - L_g \|\mathbf{x} - \mathbf{x}^*\|_1 d\mathbf{x} \\
&= Vg^* - L_g \int_{\mathcal{D}'} \|\mathbf{x} - \mathbf{x}^*\|_1 d\mathbf{x} = Vg^* - L_g \int_{[\mathbf{a}' - \mathbf{x}^*, \mathbf{b}' - \mathbf{x}^*]} \|\mathbf{x}\|_1 d\mathbf{x} \\
&= Vg^* - \\
&\quad L_g \left[\frac{1}{2} \text{vol}([\mathbf{a}' - \mathbf{x}^*, \mathbf{b}' - \mathbf{x}^*]) \sum_{i=1}^n \left(b'_i - x_i^* - (a'_i - x_i^*) + 2 \frac{(b'_i - x_i^*)(a'_i - x_i^*)}{b'_i - x_i^* - (a'_i - x_i^*)} \right) \right] \\
&= Vg^* - L_g \frac{1}{2} \text{vol}([\mathbf{a}', \mathbf{b}']) \left[\sum_{i=1}^n (b'_i - a'_i) + 2 \frac{(b'_i - x_i^*)(a'_i - x_i^*)}{b'_i - a'_i} \right] \\
&= Vg^* - \frac{L_g V}{2} \left[\|\mathbf{b}' - \mathbf{a}'\|_1 + 2 \sum_{i=1}^n \frac{(b'_i - x_i^*)(a'_i - x_i^*)}{b'_i - a'_i} \right].
\end{aligned}$$

A rearrangement gives

$$g^* \leq \frac{L_g}{2} \|\mathbf{b}' - \mathbf{a}'\|_1 + L_g \sum_{i=1}^n \frac{(b'_i - x_i^*)(a'_i - x_i^*)}{b'_i - a'_i}, \quad (12)$$

where it remains to investigate the sum. We note that $0 < b'_i - a'_i \leq \Delta_{\max}$ for all $i \in [n]$ by definition. In addition, each vertex \mathbf{v} of \mathcal{D}' is either a'_i or b'_i in its i th entry. Hence, there exists a vertex \mathbf{v} of \mathcal{D}' which attains the minimum in the inequality

$$(b'_i - x_i^*)(x_i^* - a'_i) \geq \min\{(b'_i - x_i^*), (x_i^* - a'_i)\}^2 = (v_i - x_i^*)^2,$$

for all $i \in [n]$. Using this \mathbf{v} , we can bound the sum in (12) as

$$\sum_{i=1}^n \frac{(b'_i - x_i^*)(a'_i - x_i^*)}{b'_i - a'_i} \leq -\frac{1}{\Delta_{\max}} \sum_{i=1}^n (v_i - x_i^*)^2 = -\frac{1}{\Delta_{\max}} \|\mathbf{v} - \mathbf{x}^*\|_2^2.$$

As (11) is especially true for \mathbf{v} , the assumption to be non-positive at vertices gives $0 \geq g(\mathbf{v}) \geq g^* - L_g \|\mathbf{v} - \mathbf{x}^*\|_1$ which is equivalent to $\|\mathbf{v} - \mathbf{x}^*\|_1 \geq g^*/L_g$. Combined with the well-known estimate $\sqrt{n} \|\mathbf{x}\|_2 \geq \|\mathbf{x}\|_1$, which is equivalent to $\|\mathbf{x}\|_2^2 \geq \frac{1}{n} \|\mathbf{x}\|_1^2$, we receive

$$-\frac{1}{\Delta_{\max}} \|\mathbf{v} - \mathbf{x}^*\|_2^2 \leq -\frac{1}{\Delta_{\max} n} \|\mathbf{v} - \mathbf{x}^*\|_1^2 \leq -\frac{(g^*)^2}{\Delta_{\max} n L_g^2}.$$

In summary, (12) breaks down to

$$g^* \leq \frac{L_g}{2} \|\mathbf{b}' - \mathbf{a}'\|_1 - \frac{(g^*)^2}{\Delta_{\max} n L_g},$$

which can be rearranged to

$$\frac{1}{2}(g^*)^2 + \frac{1}{2}\Delta_{\max} n L_g g^* - \frac{1}{4}\Delta_{\max} L_g^2 n \|\mathbf{b}' - \mathbf{a}'\|_1 \leq 0.$$

Solving this quadratic (in)equality for the positive solution leads to

$$\begin{aligned} g^* &\leq -\frac{1}{2}\Delta_{\max} n L_g + \sqrt{\frac{1}{4}\Delta_{\max}^2 n^2 L_g^2 + \frac{1}{2}\Delta_{\max} L_g^2 n \|\mathbf{b}' - \mathbf{a}'\|_1} \\ &\leq -\frac{1}{2}\Delta_{\max} n L_g + \sqrt{\frac{1}{4}\Delta_{\max}^2 n^2 L_g^2 + \frac{1}{2}\Delta_{\max}^2 n^2 L_g^2} \\ &= -\frac{1}{2}\Delta_{\max} n L_g + \sqrt{\frac{3}{4}\Delta_{\max}^2 n^2 L_g^2} = -\frac{1}{2}\Delta_{\max} n L_g + \frac{\sqrt{3}}{2}\Delta_{\max} n L_g \\ &= \frac{\sqrt{3}-1}{2}\Delta_{\max} n L_g, \end{aligned}$$

where we used in the second inequality that $\|\mathbf{b}' - \mathbf{a}'\|_1 \leq n\Delta_{\max}$. This gives the desired bound. \square

APPENDIX B. PARABOLIC APPROXIMATIONS – REMAINING RESULTS & PLOTS

B.1. Definition of the Zigzag Function. The zigzag function mentioned and investigated in Section 4.1 is defined by the points in Table 11, rounded to two digits for clear presentation. All x -points are sampled randomly from the uniform distribution on the interval from the previous point plus one. The function value of -5.00 is sampled uniformly on $[-1, 1]$ and every consecutive one on an interval such that the maximal slope of the zigzag function is one. The random seed in the Python implementation is two, see the repository.

x	-5.00	-4.96	-4.52	-4.19	-3.56	-3.29	-2.76	-2.24	-1.45	-0.95
$f(x)$	-0.13	-0.12	-0.19	-0.39	-0.64	-0.58	-0.97	-1.29	-0.74	-0.39
x	-0.86	-0.79	-0.68	-0.08	0.04	0.39	0.60	1.09	1.48	2.07
$f(x)$	-0.39	-0.40	-0.48	-0.81	-0.87	-0.90	-0.84	-0.83	-0.60	-1.00
x										
			2.77	3.28	3.62	4.06	4.84	5.00		
$f(x)$			-0.34	0.05	0.10	0.04	0.10	0.11		

TABLE 11. Sample points defining the zigzag function.

B.2. Number of Paraboloids for Approximating the Zigzag Function.

\mathcal{D}	ε							
	10^0	10^{-1}	10^{-2}	10^{-3}	10^0	10^{-1}	10^{-2}	10^{-3}
$[-5, -1]$	2	7	-	-	1	4	-	-
$[-2, 2]$	2	6	-	-	1	3	32	-
$[-1, 5]$	2	7	-	-	1	5	-	-
$[-5, 0]$	3	9	-	-	2	5	-	-
$[0, 5]$	3	8	-	-	1	6	-	-
$[-5, 5]$	5	-	-	-	2	10	-	-
	exact-MIP				practical-MIP			

TABLE 12. Number of paraboloids to approximate the zigzag function from above.

B.3. Number of Paraboloids for Approximating x^3 .

\mathcal{D}	ε							
	10^0	10^{-1}	10^{-2}	10^{-3}	10^0	10^{-1}	10^{-2}	10^{-3}
$[-2, 2]$	5	-	-	-	3	11	169	-
$[-5, 0]$	-	-	-	-	5	16	-	-
$[0, 5]$	-	-	-	-	4	17	-	-
$[-5, 2]$	-	-	-	-	-	-	-	-
$[-2, 5]$	-	-	-	-	-	-	-	-
$[-5, 5]$	-	-	-	-	-	-	-	-
	exact-MIP				practical-MIP			

TABLE 13. Number of paraboloids to approximate x^3 from above.

\mathcal{D}	ε							
	10^0	10^{-1}	10^{-2}	10^{-3}	10^0	10^{-1}	10^{-2}	10^{-3}
$[-2, 2]$	5	-	-	-	3	12	97	-
$[-5, 0]$	-	-	-	-	5	17	-	-
$[0, 5]$	-	-	-	-	5	17	-	-
$[-5, 2]$	-	-	-	-	-	-	-	-
$[-2, 5]$	-	-	-	-	-	-	-	-
$[-5, 5]$	-	-	-	-	-	-	-	-
	exact-MIP				practical-MIP			

TABLE 14. Number of paraboloids to approximate x^3 from below.

B.4. Plots for the Parabolic Approximations. For the zigzag function, Figure 2 visualizes the approximation results on $[-5, 5]$ from below for $\varepsilon = 10^{-1}$. In Figure 6, we visualize the latter for $\varepsilon = 10^0$ and in Figure 7 and Figure 8 the situation from above.

FIGURE 6. Approximation with $\varepsilon = 10^0$ of the zigzag function on $[-5, 5]$ from below by 2 paraboloids.

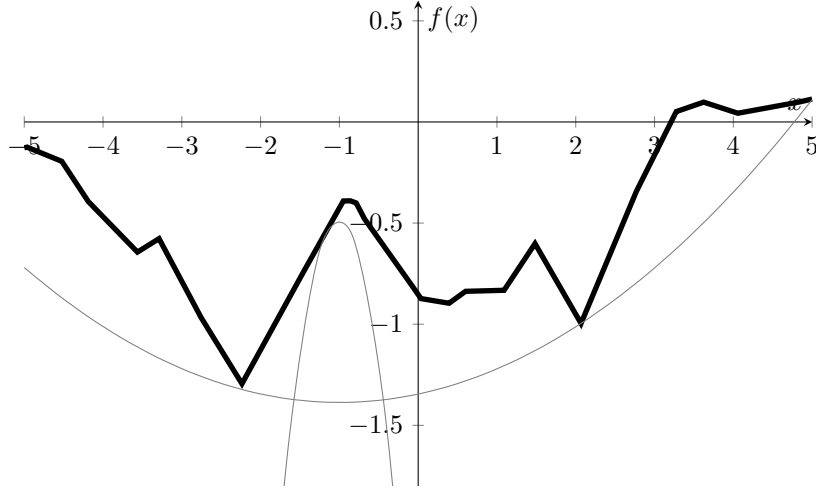


FIGURE 7. Approximation with $\varepsilon = 10^0$ of the zigzag function on $[-5, 5]$ from above by 2 paraboloids.

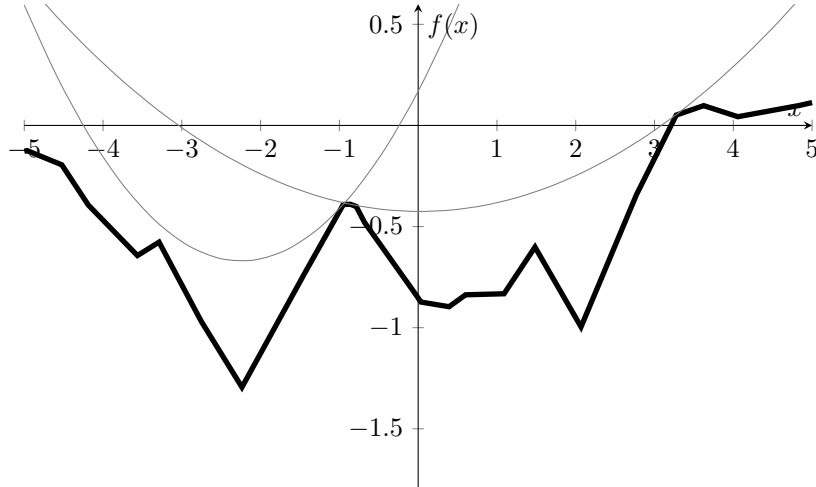
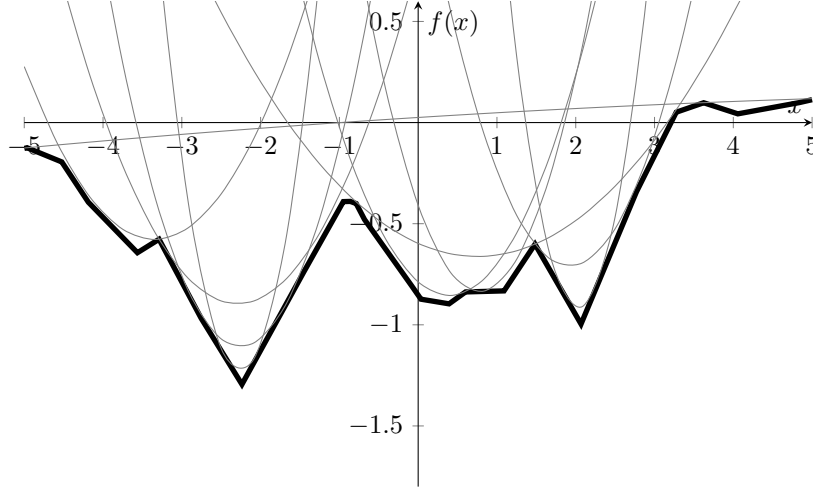


FIGURE 8. Approximation with $\varepsilon = 10^{-1}$ of the zigzag function on $[-5, 5]$ from above by 10 paraboloids.



For the sine function, we visualize its approximations on $[-\pi/2, 3\pi/2]$ from above for $\varepsilon = 10^0, 10^{-1}, 10^{-2}$ in Figures 9 to 11, respectively, and the approximations from below for $\varepsilon = 10^0, 10^{-1}$ in Figure 12 and Figure 13. The case $\varepsilon = 10^{-2}$ for the latter can be found in Figure 3.

FIGURE 9. Approximation with $\varepsilon = 10^0$ of \sin on $[-\pi/2, 3\pi/2]$ from above by 1 paraboloid.

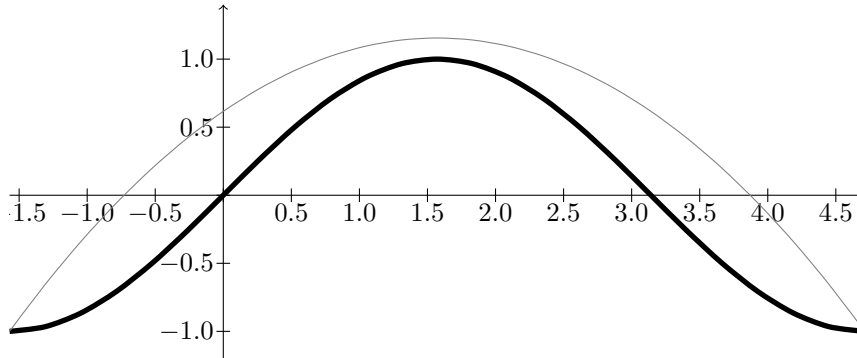


FIGURE 10. Approximation with $\varepsilon = 10^{-1}$ of \sin on $[-\pi/2, 3\pi/2]$ from above by 5 paraboloids.

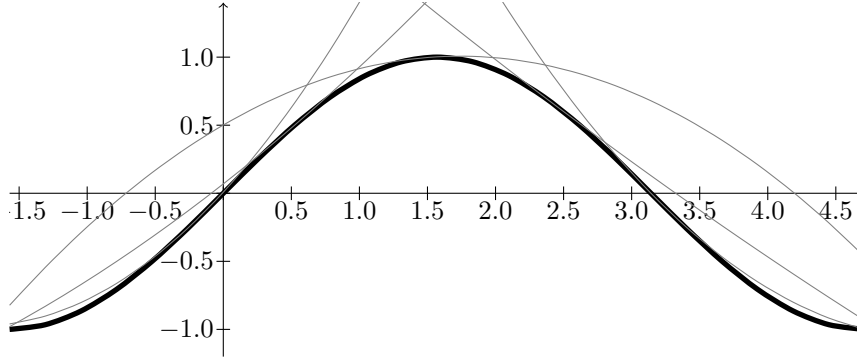


FIGURE 11. Approximation with $\varepsilon = 10^{-2}$ of \sin on $[-\pi/2, 3\pi/2]$ from above by 47 paraboloids.

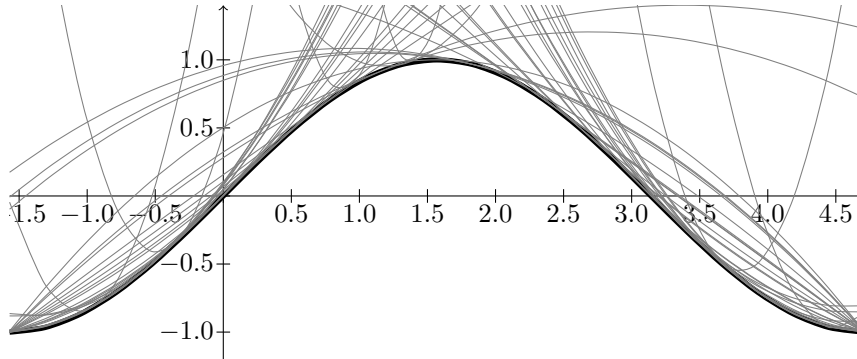


FIGURE 12. Approximation with $\varepsilon = 10^0$ of \sin on $[-\pi/2, 3\pi/2]$ from below by 1 paraboloid.

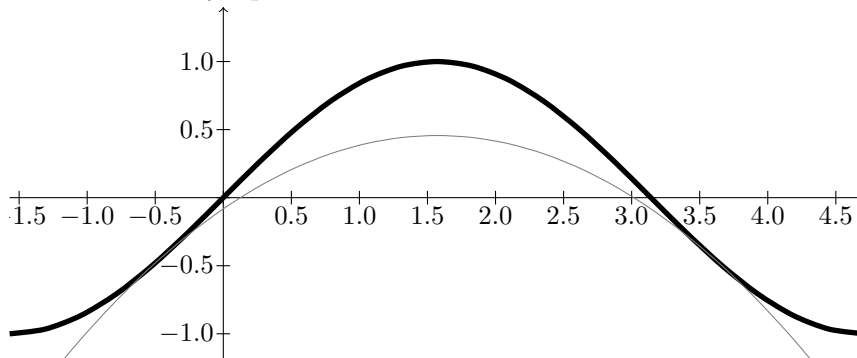
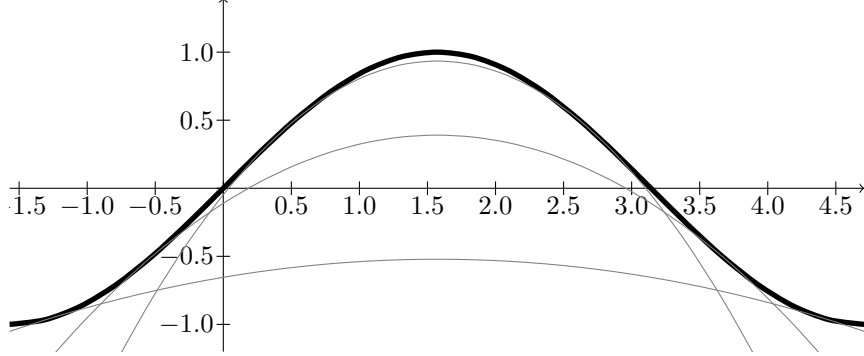


FIGURE 13. Approximation with $\varepsilon = 10^{-1}$ of \sin on $[-\pi/2, 3\pi/2]$ from below by 3 paraboloids.



The approximations for the \exp function from below on $[-2, 2]$ are summarized in Figure 14, whereas Figure 15 shows the case when approximating from above.

FIGURE 14. Approximation with $\varepsilon = 10^0, 10^{-1}, 10^{-2}$ of \exp on $[-2, 2]$ from below by 2, 4, 20 paraboloids, respectively.

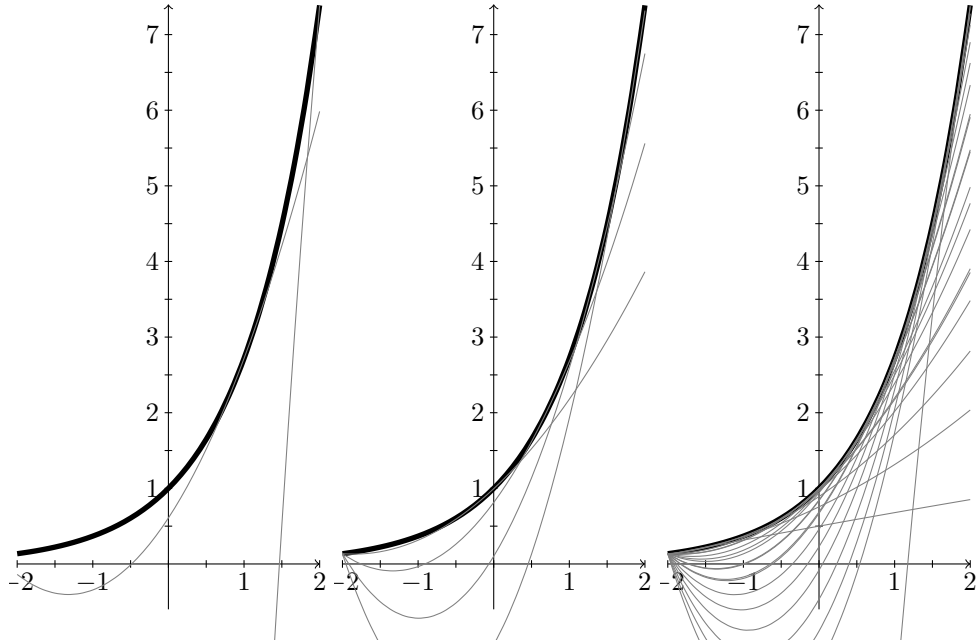
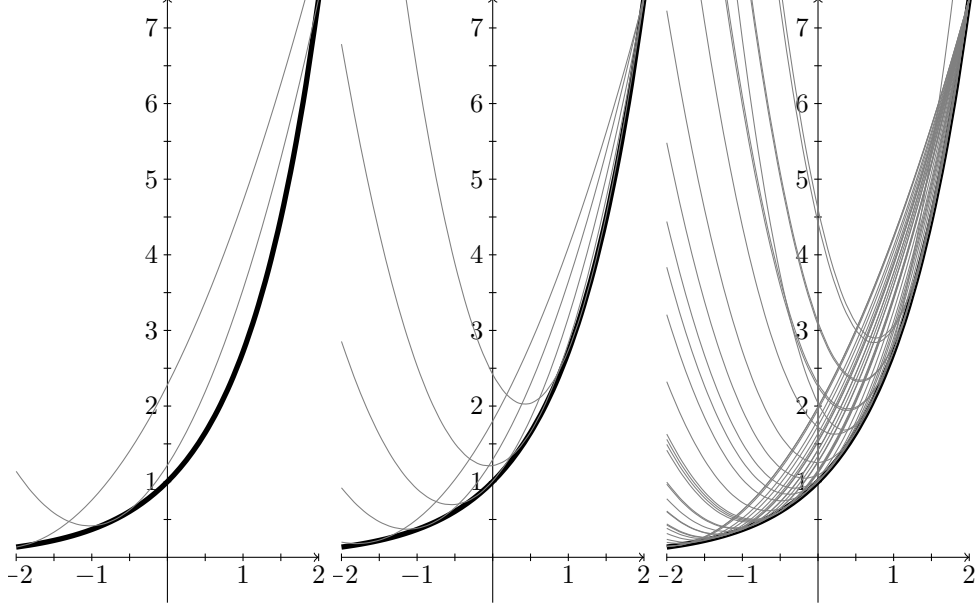
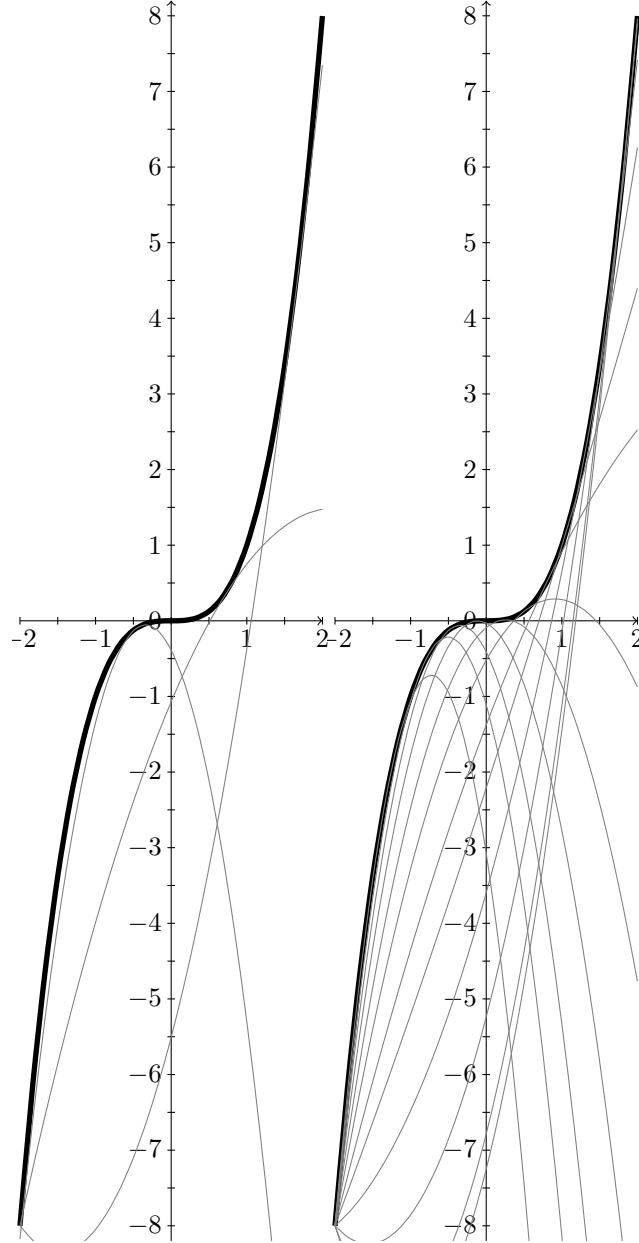


FIGURE 15. Approximation with $\varepsilon = 10^0, 10^{-1}, 10^{-2}$ of \exp on $[-2, 2]$ from above by 2, 5, 32 paraboloids, respectively.



For the approximations of x^3 on $[-2, 2]$, we restrict the visualizations to $\varepsilon = 10^0$ and $\varepsilon = 10^{-1}$, since the large number of paraboloids required for a smaller accuracy does not reveal new insights. Further, the function x^3 is point-symmetric around the origin and thus limit the plots to the approximation direction from below, see Figure 16

FIGURE 16. Approximation with $\varepsilon = 10^0, 10^{-1}$ of x^3 on $[-2, 2]$ from below by 3 and 12 paraboloids, respectively.



B.5. Overview of MINLP instances solved. In Table 15 we display an overview of the results on the MINLPLib. For the evaluations, we excluded instance ex8_4_6 for **Gurobi** and eg_disc_s for **SCIP** since they caused numerical and/or memory errors only with the respective solver. This is indicated by an asterisk.

instance	solver	type	run time in s	primal value	dual value
batchdes	Gurobi	both	0.0	167427.7	167427.7
		orig	0.0	167427.7	167427.7
		para	0.0	140933.2	140937.2
	SCIP	both	0.1	167426.7	167427.6
		orig	0.1	167427.7	167427.7
		para	0.1	140934.4	140937.1
contvar	Gurobi	both	limit	437878.5	1175110.6
		orig	limit	498872.2	inf
		para	limit	433241.9	2091301.7
	SCIP	both	limit	454624.4	809755.5
		orig	limit	538588.7	809149.8
		para	limit	459660.7	809567.8
eg_all_s	Gurobi	both	638.5	11.9	11.9
		orig	limit	1.5	7.7
		para	limit	-2.6	13.9
	SCIP	both	limit	-3.3	inf
		orig	1775.0	7.7	7.7
		para	limit	-3.7	11.6
eg_disc2_s	Gurobi	both	limit	-6.5	inf
		orig	limit	-5.2	7.0
		para	limit	-8.4	inf
	SCIP	both	limit	-7.8	inf
		orig	limit	-1.1	6.3
		para	limit	-10.6	inf
eg_disc_s	Gurobi	both	limit	-6.4	inf
		orig	limit	2.0	7.5
		para	limit	-7.8	inf
	SCIP*	both	limit	-7.7	inf
		orig	limit	3.6	5.8
		para	limit	-10.9	10.0
eg_int_s	Gurobi	both	989.0	inf	inf
		orig	limit	-1.9	inf
		para	limit	-3.1	inf
	SCIP	both	limit	-3.2	inf
		orig	9085.1	6.5	6.5
		para	limit	-3.7	inf
ex1222	Gurobi	both	0.0	1.1	1.1
		orig	0.0	1.1	1.1
		para	0.0	1.1	1.1
	SCIP	both	0.1	1.1	1.1
		orig	0.0	1.1	1.1
		para	0.0	1.1	1.1
ex14_1_3	Gurobi	both	0.2	-0.0	-0.0
		orig	0.0	-0.0	-0.0
		para	0.7	-0.0	-0.0
		both	0.1	-0.0	-0.0
	SCIP				

		orig	0.0	-0.0	-0.0
		para	0.0	-0.0	-0.0
ex14_1_4	Gurobi	both	0.2	-0.0	-0.0
		orig	0.1	-0.0	-0.0
		para	0.3	-0.0	-0.0
	SCIP	both	1.0	-0.0	-0.0
		orig	0.1	-0.0	-0.0
		para	1.0	-0.0	-0.0
ex3pb	Gurobi	both	0.0	68.0	68.0
		orig	0.0	68.0	68.0
		para	0.0	68.0	68.0
	SCIP	both	0.3	68.0	68.0
		orig	0.2	68.0	68.0
		para	0.2	68.0	68.0
ex8_1_1	Gurobi	both	0.1	-2.0	-2.0
		orig	0.0	-2.0	-2.0
		para	0.1	-2.0	-2.0
	SCIP	both	0.1	-2.0	-2.0
		orig	0.0	-2.0	-2.0
		para	0.1	-2.0	-2.0
ex8_1_2	Gurobi	both	6.2	-1.1	-1.1
		orig	2.6	-1.4	-1.4
		para	6.0	-1.1	-1.1
	SCIP	both	0.5	-1.1	-1.1
		orig	1.0	-1.1	-1.1
		para	0.3	-1.1	-1.1
ex8_2_1b	Gurobi	both	0.1	-979.2	-979.2
		orig	0.1	-979.2	-979.2
		para	0.2	-979.4	-979.4
	SCIP	both	0.6	-979.2	-979.2
		orig	0.4	-979.3	-979.2
		para	0.5	-979.4	-979.4
ex8_2_4b	Gurobi	both	0.1	-1197.2	-1197.1
		orig	0.1	-1197.2	-1197.1
		para	0.1	-1197.4	-1197.4
	SCIP	both	0.8	-1197.1	-1197.1
		orig	0.4	-1197.1	-1197.1
		para	0.7	-1197.4	-1197.4
ex8_4_6	Gurobi*	both	1.8	0.1	0.1
		orig	92.5	0.0	0.0
		para	68.0	0.6	0.6
	SCIP	both	426.3	0.0	0.0
		orig	limit	-3e+09	0.0
		para	limit	0.0	0.0
ex8_4_7	Gurobi	both	1507.3	28.9	28.9
		orig	11.0	28.8	28.8
		para	11099.4	26.9	26.9
	SCIP	both	limit	28.4	29.0
		orig	limit	25.5	29.0
		para	limit	24.3	27.0
feedtray	Gurobi	both	limit	-43.3	-13.6
		orig	limit	-45.3	inf

		para	limit	-64.1	-14.9
		both	limit	-68.6	-13.4
	SCIP	orig	limit	-68.7	-13.4
		para	limit	-68.7	-29.1
ghg_1veh	Gurobi	both	8.6	7.8	7.8
		orig	16.0	7.8	7.8
		para	10.0	7.8	7.8
	SCIP	both	14.6	7.8	7.8
		orig	19.4	7.8	7.8
		para	25.7	7.8	7.8
ghg_2veh	Gurobi	both	limit	7.5	7.8
		orig	5390.8	6.9	7.8
		para	limit	7.4	7.8
	SCIP	both	limit	7.6	7.8
		orig	limit	7.4	7.8
		para	limit	7.6	7.8
ghg_3veh	Gurobi	both	limit	6.5	7.8
		orig	limit	5.8	7.8
		para	limit	6.5	7.8
	SCIP	both	limit	6.5	7.8
		orig	limit	5.1	7.8
		para	limit	5.9	7.7
inscribedsquare01	Gurobi	both	0.9	1.0	1.0
		orig	0.4	1.0	1.0
		para	1.0	1.0	1.0
	SCIP	both	4.0	1.0	1.0
		orig	0.7	1.0	1.0
		para	4.6	1.0	1.0
inscribedsquare02	Gurobi	both	1.5	1.0	1.0
		orig	0.8	1.0	1.0
		para	3.7	1.0	1.0
	SCIP	both	6.2	1.0	1.0
		orig	1.7	1.0	1.0
		para	15.1	1.0	1.0
inscribedsquare03	Gurobi	both	2.2	23.8	23.8
		orig	1.2	23.8	23.8
		para	2.9	24.0	24.0
	SCIP	both	11.6	23.8	23.8
		orig	4.5	23.8	23.8
		para	15.8	24.0	24.0
kriging_peaks-red020	Gurobi	both	14.4	0.4	0.4
		orig	4.0	0.4	0.4
		para	14.2	0.4	0.4
	SCIP	both	31.3	0.4	0.4
		orig	773.7	0.4	0.4
		para	19.2	0.4	0.4
Ints100	Gurobi	both	limit	0.6	0.6
		orig	limit	0.5	0.6
		para	limit	0.6	0.8
	SCIP	both	limit	0.6	0.6
		orig	limit	0.5	0.6
		para	3889.5	0.6	0.6

lnts200	Gurobi	both	limit	0.5	inf
		orig	limit	0.5	0.6
		para	limit	0.6	0.6
	SCIP	both	limit	0.5	0.6
		orig	limit	0.5	0.6
		para	limit	0.5	0.6
lnts400	Gurobi	both	limit	0.5	inf
		orig	limit	0.5	0.6
		para	limit	0.6	0.7
	SCIP	both	limit	0.5	inf
		orig	limit	0.5	0.6
		para	limit	0.5	inf
lnts50	Gurobi	both	13371.4	0.6	0.6
		orig	5811.5	0.6	0.6
		para	limit	0.6	0.6
	SCIP	both	limit	0.6	0.6
		orig	limit	0.5	0.6
		para	51.1	0.6	0.6
mathopt6	Gurobi	both	0.2	-3.3	-3.3
		orig	0.1	-3.3	-3.3
		para	0.1	-3.3	-3.3
	SCIP	both	1.5	-3.3	-3.3
		orig	0.5	-3.3	-3.3
		para	0.5	-3.3	-3.3
polygon100	Gurobi	both	limit	-1.6	-0.7
		orig	limit	-1.6	-0.8
		para	limit	-2.2	-0.8
	SCIP	both	limit	-1.6	0.0
		orig	limit	-26.6	-0.8
		para	limit	-43.9	-0.1
polygon25	Gurobi	both	limit	-1.6	-0.7
		orig	limit	-1.6	-0.8
		para	limit	-1.9	-0.7
	SCIP	both	limit	-1.4	-0.7
		orig	limit	-4.4	-0.8
		para	limit	-1.9	-0.7
polygon50	Gurobi	both	limit	-1.6	-0.7
		orig	limit	-1.6	-0.8
		para	limit	-2.1	-0.8
	SCIP	both	limit	-1.6	-0.7
		orig	limit	-10.4	-0.8
		para	limit	-2.8	-0.8
polygon75	Gurobi	both	limit	-1.6	-0.7
		orig	limit	-1.6	-0.8
		para	limit	-2.2	-0.8
	SCIP	both	limit	-1.6	0.0
		orig	limit	-17.4	-0.8
		para	limit	-3.1	-0.9
pooling_epa1	Gurobi	both	8.6	-280.8	-280.8
		orig	3.6	-280.8	-280.8
		para	6.1	-291.8	-291.7

	SCIP	both	142.1	-280.8	-280.8
		orig	53.9	-280.8	-280.8
		para	9.4	-291.8	-291.7
pooling_epa2	Gurobi	both	126.6	-4567.7	-4567.4
		orig	224.9	-4567.7	-4567.3
		para	102.1	-4567.6	-4567.2
	SCIP	both	2797.2	-4567.4	-4567.4
		orig	limit	-4637.3	-4567.4
		para	2047.9	-4567.7	-4567.4
pooling_epa3	Gurobi	both	limit	-14998.5	-14961.6
		orig	limit	-14998.6	-14963.5
		para	limit	-14998.6	-14963.0
	SCIP	both	limit	-14998.6	inf
		orig	limit	-14998.6	-14936.8
		para	limit	-14998.6	-14535.8
synthes2	Gurobi	both	0.1	73.0	73.0
		orig	0.0	73.0	73.0
		para	0.1	72.9	72.9
	SCIP	both	0.2	73.0	73.0
		orig	0.1	73.0	73.0
		para	0.6	72.9	72.9
synthes3	Gurobi	both	0.1	68.0	68.0
		orig	0.0	68.0	68.0
		para	0.0	68.0	68.0
	SCIP	both	0.3	68.0	68.0
		orig	0.2	68.0	68.0
		para	0.3	68.0	68.0
t1000	Gurobi	both	1.5	0.0	0.0
		orig	1.3	0.0	0.0
		para	0.5	0.0	0.0
	SCIP	both	0.2	0.0	0.0
		orig	915.5	-0.0	-0.0
		para	0.6	0.0	0.0

TABLE 15. Overview of all MINLPLib instances solved.